DEVELOPMENT OF AN APPROACH TO MODELING LOADING AND ELUTION OF SPHERICAL RESORCINOL FORMALDEHYDE ION-EXCHANGE RESIN

S. E. Aleman
L. L. Hamm
F. G. Smith, III

SEPTEMBER, 2011

Savannah River National Laboratory
Savannah River Nuclear Solutions
Savannah River Site
Aiken, SC 29808

Prepared for the U.S. Department of Energy Under Contract Number DE-AC09-08SR22470

SRNL™

DISCLAIMER

Printed in the United States of America

Prepared For

U.S. Department of Energy

Key Words:
Ion Exchange
Resorcinol-Formaldehyde Resin
Isotherm Modeling
Column Modeling

Retention:
Permanent

DEVELOPMENT OF AN APPROACH TO MODELING LOADING AND ELUTION OF SPHERICAL RESORCINOL FORMALDEHYDE ION-EXCHANGE RESIN

S. E. Aleman
L. L. Hamm
F. G. Smith, III

SEPTEMBER, 2011

Savannah River National Laboratory
Savannah River Nuclear Solutions
Savannah River Site
Aiken, SC 29808

Prepared for the U.S. Department of Energy Under
Contract Number DE-AC09-08SR22470

SRNL™

REVIEWS AND APPROVALS

Authors

_____

S. E. Aleman, Threat Assessments Date

_____

L. L. Hamm, Process Modeling and Computational Chemistry Date

_____

F. G. Smith, III, Process Modeling and Computational Chemistry Date

Technical Review

_____

W. D. King, Advanced Characterization and Process Development Date

Approval

_____

S. J. Hensel, Manager, Process Modeling and Computational Chemistry Date

_____

F. M. Pennebaker, Manager, Advanced Characterization and Process Development Date

TABLE OF CONTENTS

TABLE OF FIGURES

TABLE OF TABLES

LIST OF ACRONYMS

CSTR	Continuous Stirred Tank Reactor
DF	Diluted Feed
ORNL	Oak Ridge National Laboratory
PNWD	Pacific Northwest Division
sRF	Spherical Resorcinol Formaldehyde
SCIX	Small Column Ion Exchange
SRNL	Savannah River National Laboratory
SRS	Savannah River Site
WTP	Waste Treatment Plant

1.0 Executive Summary

Ion-exchange modeling work performed in FY2011 focused on the development of isotherms and column modeling techniques that would allow prediction of a complete ion-exchange cycle for elutable polyfunctional ion-exchange resins. The immediate application of interest is cesium removal from radioactive salt solutions using spherical Resorcinol Formaldehyde (sRF) followed by elution of the cesium from the resin. It is expected that this will be implemented in the Small Column Ion-Exchange (SCIX) process at Hanford and in the Hanford Waste Treatment Plant (WTP). Excluding column pretreatment steps, which will be considered in future modeling efforts, a complete ion-exchange cycle consists of:

- Column loading where cesium ions are removed from caustic feed solution and retained on the ion-exchange resin.
- Feed solution displacement and column rinsing where feed solution remaining in the ion-exchange bed after loading is flushed out of the column and the column is rinsed with a mildly caustic or near neutral solution.
- Column elution where cesium ions are removed from the ion-exchange resin and redissolved by passing an acidic solution through the column.

Note that a multi-column carousel configuration is employed where the lead column is taken out of the carousel for elution each cycle. During a single cycle the above process results in aqueous phase shifts in pH from approximately 1 or lower to 14 or higher. Recent scoping titration data (Nash and Polite, 2011) indicate that sRF is a polyfunctional resin whose rings contain fixed ionogenic acid groups of the following types:

a. Sulfonic (SO_3H) groups with pK_a values probably within the range 0-1;
b. Carboxylic (COOH) groups with pK_a values probably within the range 5-8; and
c. Resorcylic (OH) groups with pK_a values probably within the range 9-12.

Figure 1.1 shows sRF sodium uptake data (taken at SRNL and ORNL) over a wide range of pH conditions along with predictions made using a very simple multi-site deprotonation model. The predictions shown are based on the assumption of three different ring types. The presence of such a mixture of strong, weak, and very weak acid groups can play a significant role in the overall performance of a resin. It is believed that the majority of available exchange sites are of the resorcylic group type, while non-trivial amounts of the other two exchange groups are most likely present.

Prior to the FY2011 modeling effort, ion-exchange modeling has primarily focused on prediction of cesium loading and determining the point of breakthrough when the loading phase of the ion-exchange cycle should be terminated. At these high pH conditions virtually all of the ionogenic groups are disassociated and contribute to the overall resin exchange capacity. Given the expected ionic group makeup, cesium selectivity is probably dominated by the resorcylic groups. However, at pH conditions under 4, such as the elution step, only the sulfonic groups would be potentially active and play a role in performance associated with solution pH and cationic selectivities. Prior experimental results have demonstrated that sRF resin can effectively remove cesium during elution using 0.5 M HNO_3. In these studies varying and sometimes persistent tailing of the elution curves exist. More recent studies (Brown et al., 2011) indicate that cesium removal using more dilute HNO_3 is possible. Based on the prior experimental studies and the

desire to consider process baseline changes, it is recognized that modeling of the elution process can assist in process optimization studies.

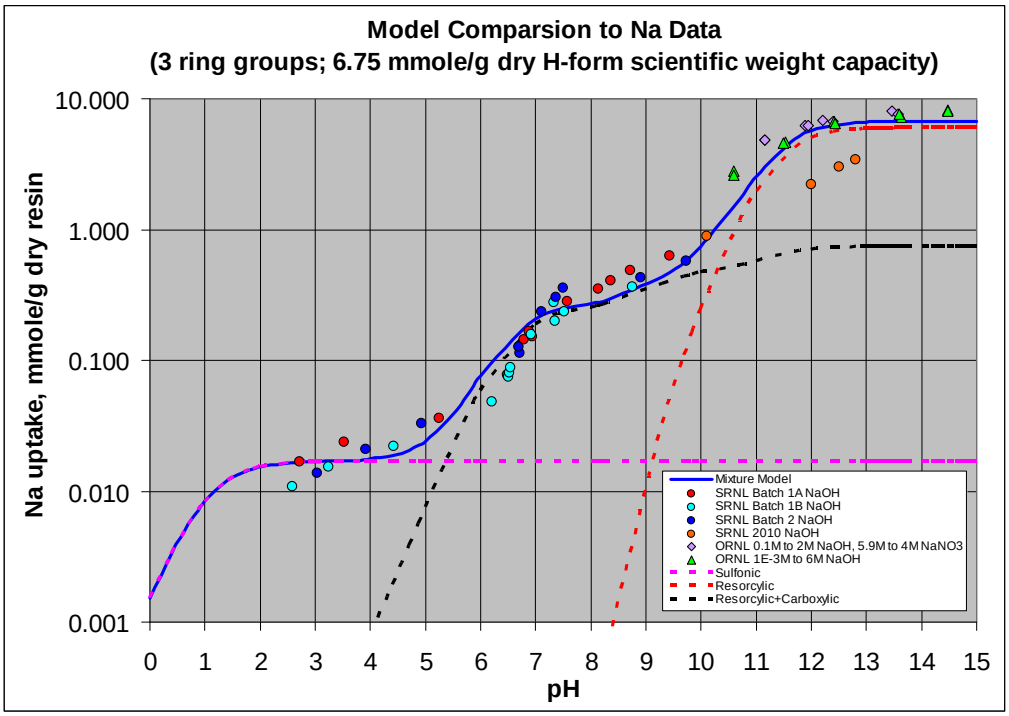

Figure 1.1 Scoping titration data (Nash and Polite, 2011) for spherical resorcinol formaldehyde resin (batch 641) illustrating its polyfunctional behavior.

Given the more recent understanding with regard to the polyfunctional behavior of sRF, a fundamental shift in our general approach to ion-exchange modeling has occurred. In prior SRNL efforts column loading performance was computed using the VERSE-LC liquid chromatography algorithm (Whitley and Wang, 1998) where local reaction kinetics was assumed infinite (i.e., assumed solid-liquid equilibrium based on a single or multi-component Langmuir or Freundlich/Langmuir isotherm). For monovalent cation exchange these semi-empirical isotherms are equivalent to mass action equilibrium equations. To extend our analysis using VERSE to address the entire range of pH conditions, the mass action kinetics equations for monovalent cation exchange were employed (Ernest et al., 1997). Numerical testing has demonstrated that VERSE using this non-equilibrium option can numerically handle very large concentration shifts observed over the entire range of process conditions.

The basic concept is to numerically simulate the entire series of ion-exchange process steps by breaking up the entire pH range into several much smaller ranges. Within each of these small pH ranges multi-component mass action equilibrium equations are derived and then converted into their appropriate kinetic forms. Then a series of sequential VERSE runs would be made for each small pH range. Work conducted in FY2011 has started development of the thermodynamic ion-exchange model and demonstrated column calculations using the mass-action kinetic equation approach (both agreed qualitatively with experimental data). When fully developed, this model should be able to accurately predict column loading and elution while accounting for high salt concentrations (Na^+ and K^+) thus allowing simulation of complete ion-exchange cycles.

2.0 Introduction

The current strategy for removal of cesium from the Hanford waste stream is ion-exchange using spherical Resorcinol-Formaldehyde (sRF) resin. The original resin of choice was granular SuperLig 644 resin and during testing of this resin several operational issues were identified. For example, the granular material had a high angle of internal friction resulting in fragmentation of resin particles along its edges during cycling and adverse hydraulic performance. Efforts to replace SuperLig 644 were undertaken and one candidate was the granular Resorcinol-Formaldehyde (RF) resin where experience with this cation exchanger dates back to the late 1940's. To minimize hydraulic concerns a spherical version of RF was developed and several different chemically produced batches were created. The 5E-370/641 batch of sRF was selected and for the last decade numerous studies have been performed (e.g., batch contact tests, column loading and elution tests).

The WTP flowsheet shows that the aqueous phase waste stream will have a wide range of ionic concentrations (e.g., during the loading step 0-3 M free OH, 5+ M Na, 0-1 M K, 0-3 M NO_3 …). Several steps are required in the ion-exchange process to achieve the required Cs separation factors: loading, displacement, washing, elution, and regeneration. The sRF resin will be operated over a wide range in pH (i.e., pH of 12-14 during the loading step and pH of 0.01-1 during the elution step). During some of these steps very high levels of counter-ions and co-ions will be present within the aqueous phase. Alternative process feeds are under consideration as well (e.g., sodium levels as high as 8 M and column operation up to 45 C during loading, reduced and recycled HNO_3 during elution).

In order to model the performance of sRF resin through an entire ion-exchange cycle, a more robust isotherm model is required. To achieve this more robust isotherm model requires knowledge of the numbers and kinds of fixed ionogenic groups that make up sRF. Recent literature reviews and scoping titration tests strongly indicate that sRF is a polyfunctional cation exchange resin with at least three dominant types of ring groups playing a role in its isotherm behavior over the wide pH range of operations. Also three types of fixed ionogenic acid groups are present: sulfonic (SO_3H^-) groups; carboxylic ($COOH^-$) groups, and resorcylic (OH^-) groups. It is this premise that we are working under in the development of a robust isotherm model for sRF over its entire planned pH operating range.

The application of prototypic isotherms for modeling ion-exchange column behavior is demonstrated in Section 3 of this report. This preliminary work served to focus the development effort on the use of a mass-action based isotherm. In Section 4 of this report, the foundational material required to develop a robust isotherm model for sRF is provided. The paths taken, and choices made, are given for the reader to better understand our current status with respect to this goal and to highlight our most recent understanding of sRF exchange equilibria. Our ultimate goal is to update the CERMOD code (Aleman and Hamm, 2007) with a robust isotherm model for sRF that spans the entire pH and concentration ranges of planned operations. The isotherm model will then be used in the VERSE-LC code to model an entire ion-exchange cycle.

3.0 Column Modeling

For the past 10 years, SRNL has been using the VERSE-LC code developed at Purdue University (Whitley and Wang, 1998., Berninger et al., 1991) to model the performance of ion-exchange columns. VERSE-LC provides a one-dimensional model of flow and transport through a packed bed coupled with a one-dimensional model of transport and ion-exchange within the particle pores. While using a commercial code has some limitations, we have found VERSE-LC to be generally satisfactory for modeling ion-exchange processes for several different resins at the Savannah River Site (Smith, 2007) and the Hanford Waste Treatment Plant (Aleman et al., 2007). At both sites, the primary application has been cesium removal from caustic salt solutions. VERSE-LC offers a wide choice of isotherms that can be used to describe the ion-exchange process.

Until this year, column modeling at SRNL has typically been limited to describing column loading and predicting the breakthrough point to assist in designing ion-exchange processes. However, with the use of elutable ion-exchange resins such as sRF, there is also interest in modeling the entire ion-exchange cycle which consists of the following steps: 1) Loading the resin with cesium by passing salt solution through the column, 2) Displacing the feed solution and washing the loaded column, and 3) Eluting cesium from the resin with an acidic solution. The work performed in 2011 focused on methods to model the entire ion-exchange cycle.

3.1 Freundlich/Langmuir Isotherms

As noted above, VERSE-LC provides a relatively extensive suite of ion-exchange isotherms to use for column modeling. Previous work at SRNL has primarily used single component isotherms to describe cesium loading on an ion-exchange column. The simplest example of this isotherm is the single component Langmuir form shown in Eq. (3.1):

$$Q_{Cs} = \frac{a\, C_{Cs}}{\beta + b\, C_{Cs}} \tag{3.1}$$

In Eq. (3.1), Q_{Cs} is the cesium loading on the solid phase, C_{Cs} is the cesium concentration in the fluid phase and a, b and β are constants whose values are determined by fitting to experimental data. To obtain an improved fit to experimental data, particularly at low cesium concentrations, the single component Freundlich/Langmuir isotherm shown in Eq. (3.2) has also been used.

$$Q_{Cs} = \frac{a\, C_{Cs}^{Ma}}{\beta + b\, C_{Cs}^{Mb}} \tag{3.2}$$

In Eq. (3.2), the additional constants M_a and M_b are introduced which can be used to better fit data. However, Eq. (3.2) is not thermodynamically consistent.

In the applications of interest, the cesium is being removed from a salt solution that contains other monovalent ions such as sodium, potassium, and rubidium that can compete with cesium for ion-exchange sites on the resin. VERSE-LC also allows the use of multicomponent versions of Eq. (3.1) and Eq. (3.2). For example a three component version of Eq. (3.2) for the system of Cs^+, Na^+ and H^+ would consist of the set of equations:

$$Q_{Cs} = \frac{a_{Cs}\, C_{Cs}^{M_{a,Cs}}}{\beta_{Cs} + b_{Cs}\, C_{Cs}^{M_{b,Cs}} + b_{Na}\, C_{Na}^{M_{b,Na}} + b_H\, C_H^{M_{b,H}}} \tag{3.3a}$$

$$Q_{Na} = \frac{a_{Na}\, C_{Na}^{M_{a,Na}}}{\beta_{Na} + b_{Cs}\, C_{Cs}^{M_{b,Cs}} + b_{Na}\, C_{Na}^{M_{b,Na}} + b_H\, C_H^{M_{b,H}}} \quad (3.3b)$$

$$Q_H = \frac{a_H\, C_H^{M_{a,H}}}{\beta_H + b_{Cs}\, C_{Cs}^{M_{b,Cs}} + b_{Na}\, C_{Na}^{M_{b,Na}} + b_H\, C_H^{M_{b,H}}} \quad (3.3c)$$

Equations (3.3a) – (3.3c) are a straight forward extension of Eq (3.2) expanded to include adsorption terms for all of the ions and corresponding ion specific constants. In Eq. (3.1) and Eq. (3.2), the β parameter can be set equal to one without any loss of generality. In Eqs. (3.3a) – (3.3c), the β terms can be thought of as representing effects from additional ions, such as K^+ or Rb^+, that are not explicitly modeled.

The experience at SRNL using multicomponent isotherms in VERSE-LC has been that the model can sometimes run very slowly compared to the single component isotherm models. During column loading, the ion-exchange resins typically quickly reach equilibrium with the sodium and potassium ions in solution and the single component isotherm provides an accurate approximation for cesium ion-exchange. However, the initial attempt to model column elution as well as loading used the three component isotherm model shown in Eqs. (3.3a) – (3.3c). The thought was that an equation for the hydrogen ion exchange should be included in order to model elution behavior. The hydrogen ion term would be insignificant during column loading, when the H^+ concentration in solution is negligible, but would be significant during elution with an acidic solution where the H^+ concentration would be very large relative to that of Cs^+. During elution, the hydrogen ion term in the denominator of Eq. (3.3a) would force the cesium concentration on the resin to a small value. Model parameter values shown in Table 3.1 were used for a set of trial calculations. The cesium parameters were derived from the existing SRNL thermodynamic model of sRF ion-exchange. However, the parameters for sodium and hydrogen are arbitrarily chosen and simply intended to demonstrate model behavior.

Table 3.1 Parameter values for three component Freundlich/Langumir isotherm.

	H^+	Na^+	Cs^+
a	1.0	0.1	410.0
b	250.0	0.2	2000.0
M_a	1.0	1.0	0.9717
M_b	1.0	1.0	0.9044
β	0	0	0

The multicomponent isotherm model was run in VERSE-LC to simulate recent experiments conducted at ORNL demonstrating cesium elution from a sRF column (Taylor and Johnson, 2009). Unfortunately, the experiments did not achieve cesium saturation of the column during loading. However, the multicomponent isotherm produced the same resin loading as that calculated with the single component cesium isotherm usually used to model such experiments. Figures 3.1 and 3.2 show the elution behavior predicted by the multicomponent model in 0.5 and 0.1 M HNO_3, respectively compared to ORNL experimental data. While the model is able to predict cesium elution, the timing and shape of the observed elution curves are not accurately modeled. Definition of the experimental curve is limited by the necessity of collecting discrete samples. The instantaneous model result shows tall sharp peaks but the experiment cannot measure this because the effluent sample is approximately one column volume which reduces peak sharpness.

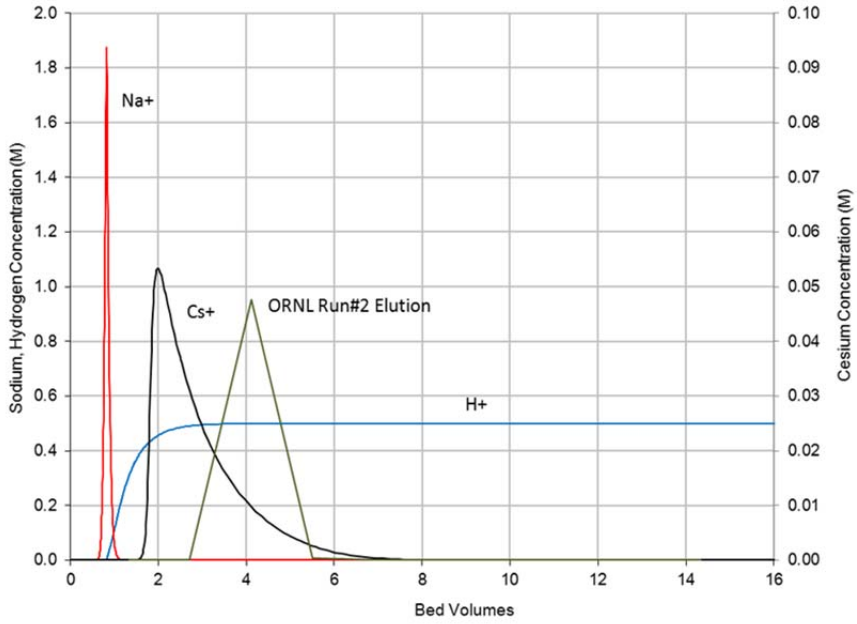

Figure 3.1 Multicomponent isotherm model prediction of cesium elution during ORNL elution Run #2 using 0.5 M HNO_3.

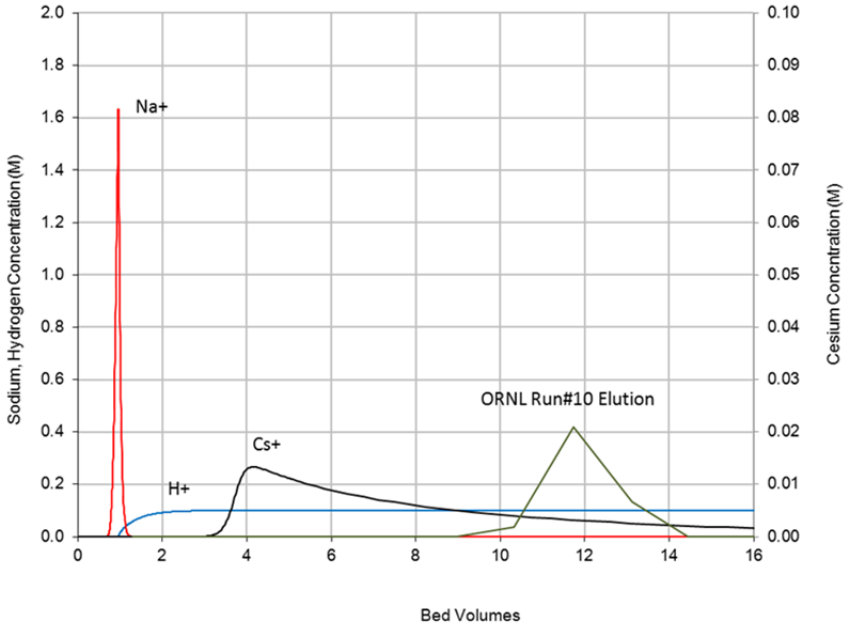

Figure 3.2 Multicomponent isotherm model prediction of cesium elution during ORNL elution Run #10 using 0.1 M HNO_3.

3.2 pH Dependent Separation Factor Isotherm

A second approach investigated to modeling both loading and elution on sRF ion-exchange columns used the following pH dependent isotherm available in VERSE-LC:

$$\boldsymbol{Q_i} = \frac{\boldsymbol{\alpha_{i,1}}\, \boldsymbol{c_i}\, \overline{\boldsymbol{C}}_{\boldsymbol{T}}}{\sum_{j=1}^{N_c} \boldsymbol{\alpha_{j,1}}\, \boldsymbol{c_j}} \tag{3.4}$$

$$\boldsymbol{\alpha_{i,1}(pH)} = \frac{\boldsymbol{k_{1,i}} + \boldsymbol{k_{2,i}} 10^{\left(pH - pKa_{1,i}\right)} + \boldsymbol{k_{3,i}} 10^{\left(pH - pKa_{2,i}\right)} + \boldsymbol{k_{4,i}} 10^{\left(2\,pH - pKa_{1,i} - pKa_{2,i}\right)}}{1 + 10^{\left(pH - pKa_{1,i}\right)} + 10^{\left(pH - pKa_{2,i}\right)} + 10^{\left(2\,pH - pKa_{1,i} - pKa_{2,i}\right)}} \tag{3.5}$$

In these equations:

$\boldsymbol{Q_i}$ .....Concentration of species i on solid phase (mol/gram or mol/BV),

$\boldsymbol{c_i}$ .....Concentration of species i in liquid phase (mol/liter),

$\overline{\boldsymbol{C}}_{\boldsymbol{T}}$ .....Total ion-exchange capacity of solid (mol/gram or mol/BV),

$\boldsymbol{\alpha_{i,1}}$ .....Separation factor for species i relative to species 1,

$\boldsymbol{N_c}$ .....Number of components,

$\boldsymbol{k_{1,i}}$ .....Constant for species i,

$\boldsymbol{pKa_{1,i}}, \boldsymbol{pKa_{2,i}}$ .....Acid dissociation constants for species i (sRF is believed to contain two exchangeable sites with pKa values approximately the same as those of resorcinol).

The pH is calculated based on the concentration of the first component. Therefore, species number 1 must represent the H^+ ion. Terms in the denominator of Eq. (3.5) are added only if the corresponding term in the numerator has a non-zero $\boldsymbol{k}$ coefficient. Therefore, if $\boldsymbol{k}_{3,i}$ and $\boldsymbol{k}_{4,i}$ are set equal to zero, Eq. (3.5) reduces to:

$$\boldsymbol{\alpha_{i,1}(pH)} = \frac{\boldsymbol{k_{1,i}} + \boldsymbol{k_{2,i}} 10^{\left(pH - pKa_{1,i}\right)}}{1 + 10^{\left(pH - pKa_{1,i}\right)}} \tag{3.6a}$$

If only $\boldsymbol{k}_{4,i}$ is set equal to zero, Eq. (3.5) reduces to:

$$\boldsymbol{\alpha_{i,1}(pH)} = \frac{\boldsymbol{k_{1,i}} + \boldsymbol{k_{2,i}} 10^{\left(pH - pKa_{1,i}\right)} + \boldsymbol{k_{3,i}} 10^{\left(pH - pKa_{2,i}\right)}}{1 + 10^{\left(pH - pKa_{1,i}\right)} + 10^{\left(pH - pKa_{2,i}\right)}} \tag{3.6b}$$

The above equations are attractive since they have a built in dependence on solution pH. Weak acid cation exchange resins load at high pH and elute at low pH; therefore, it was thought possible that these isotherms could be used to model the behavior of sRF over the entire operating range. However, there are two problems with using this isotherm to model sRF loading and elution.

1. As shown below, Eq. (3.4) can be manipulated into the form of a Langmuir isotherm but it cannot emulate the Freundlich/Langmuir isotherm which has been used to better fit sRF

loading data at low cesium concentrations. In fact, no other VERSE-LC isotherm can be transformed into the Freundlich/Langmuir form.

2. Because the term that appears in the transport model equations is actually the derivative of the isotherm, VERSE-LC does not store solid phase concentrations. This precludes using one isotherm, such as Freundlich/Langmuir, to model adsorption and then switching to another isotherm, such as the Separation Factor isotherm shown above, to model elution. Since VERSE-LC recalculates the solid concentration at each time step, switching isotherms does not conserve the amount of adsorbed species.

As noted above, the first species in the Separation Isotherm model must be H^+ which is used to calculate the pH. The second species in our model is chosen to be Cs^+ and, to allow emulation of a Langmuir isotherm, we also introduce an arbitrary third species called X. It may be possible to define X as an actual solution species such as Na^+ or NO_3^- and use it to model some aspect of the ion-exchange behavior. However, for this initial evaluation, we will define X as some undefined arbitrary species. The separation factors are intended to be relative to the first species (H^+) although this is not an actual constraint on the VERSE-LC input. For these three species, Eq. (3.4) becomes:

$$\boldsymbol{Q}_H = \frac{\boldsymbol{\alpha}_H \boldsymbol{c}_H \overline{\boldsymbol{C}}_T}{\boldsymbol{\alpha}_H \boldsymbol{c}_H + \boldsymbol{\alpha}_{Cs} \boldsymbol{c}_{Cs} + \boldsymbol{\alpha}_X \boldsymbol{c}_X} \tag{3.7a}$$

$$\boldsymbol{Q}_{Cs} = \frac{\boldsymbol{\alpha}_{Cs} \boldsymbol{c}_{Cs} \overline{\boldsymbol{C}}_T}{\boldsymbol{\alpha}_H \boldsymbol{c}_H + \boldsymbol{\alpha}_{Cs} \boldsymbol{c}_{Cs} + \boldsymbol{\alpha}_X \boldsymbol{c}_X} \tag{3.7b}$$

$$\boldsymbol{Q}_X = \frac{\boldsymbol{\alpha}_X \boldsymbol{c}_X \overline{\boldsymbol{C}}_T}{\boldsymbol{\alpha}_H \boldsymbol{c}_H + \boldsymbol{\alpha}_{Cs} \boldsymbol{c}_{Cs} + \boldsymbol{\alpha}_X \boldsymbol{c}_X} \tag{3.7c}$$

For trial purposes, we assumed that all of the $\boldsymbol{k}_{3,i}$ and $\boldsymbol{k}_{4,i}$ terms were zero so Eq. (3.5) reduced to Eq. (3.6a). Further, we assumed that $\boldsymbol{k}_{1,H}$ =1 and $\boldsymbol{k}_{2,H}$ =0 so that $\boldsymbol{\alpha}_H$ = 1 as intended.

Column loading occurs at high pH where the liquid concentration of H^+ is very low (~ 10^{-14}). In this case, the H^+ terms are negligible and the above equations reduce to:

$$\boldsymbol{Q}_{Cs} = \frac{\boldsymbol{\alpha}_{Cs} \boldsymbol{c}_{Cs} \overline{\boldsymbol{C}}_T}{\boldsymbol{\alpha}_{Cs} \boldsymbol{c}_{Cs} + \boldsymbol{\alpha}_X \boldsymbol{c}_X} \tag{3.8a}$$

$$\boldsymbol{Q}_X = \frac{\boldsymbol{\alpha}_X \boldsymbol{c}_X \overline{\boldsymbol{C}}_T}{\boldsymbol{\alpha}_{Cs} \boldsymbol{c}_{Cs} + \boldsymbol{\alpha}_X \boldsymbol{c}_X} \tag{3.8b}$$

As a test case, the ORNL 2008 small column experiment (Taylor and Johnson, 2009) was modeled. This experiment involved a 20 ml column operating at 25 C with a feed flow rate of 0.6 ml/min. Using a thermodynamic model of sRF ion-exchange developed at SRNL (Aleman and Hamm, 2007), coefficients for a Langmuir isotherm for this experiment were estimated to be:

$$\boldsymbol{Q}_{Cs} = \frac{0.1717 \boldsymbol{c}_{Cs}}{3.316\text{x}10^{-4} + \boldsymbol{c}_{Cs}} \tag{3.9}$$

Dividing the numerator and denominator in Eq. (3.9) by the $\boldsymbol{\beta}$ term ($3.316\text{x}10^{-4}$) gives:

$$Q_{Cs} = \frac{3015.7\, c_{Cs}\ 0.1717}{1 + 3015.7\, c_{Cs}} \tag{3.10}$$

To correspond to the form of Eq. (3.8a), we set $\alpha_{Cs} = 3015.7$ and $\overline{C}_T = 0.1717$. Typically, c_{Cs} is on the order of 10^{-3} to 10^{-8}, so the factor of one in the denominator of Eq. (3.10) is a significant term. That is why the additional X species is included in the model. To accurately simulate sRF loading, the term $\alpha_X\, c_X$ in the denominator of Eq. (3.8a) must equal one. To a close approximation, this can be accomplished by setting $k_{1,X}$ =1 and $k_{2,X}$ =0 so that α_X = 1 while setting the initial concentration of species X to 1.0 and the concentration in the column feed to 1.0 as well. The loading model, where c_0 is the initial concentration and c_f is the feed concentration, is then defined by the following set of coefficients:

$\overline{C}_T$ = 0.1717

$\alpha_{H,1}$ = 1	$c_{0,H} = 10^{-12}$	$c_{f,H} = 10^{-12}$
$\alpha_{Cs,1}$ = 3015.7	$c_{0,Cs}$ = 0	$c_{f,Cs} = 1.90\text{x}10^{-3}$
$\alpha_{X,1}$ = 1	$c_{0,X}$ = 1.0	$c_{f,X}$ = 1.0

When the hydrogen ion concentration is zero, VERSE-LC sets the pH equal to 14. Testing showed that the code ran poorly when the H^+ concentration was identically zero so the small value of 10^{-12} was used instead. The formulation shown above gave column loading results comparable to those obtained using a Langmuir isotherm. However, before proceeding to the discussion of results, we will first examine using the pH dependent terms in the separation factor isotherm to model column elution.

To model the elution of Cs^+ from the sRF resin we assume that the Cs^+ isotherm has the pH dependence of Eq. (3.6a):

$$\alpha_{Cs,1}(pH) = \frac{k_{1,Cs} + k_{2,Cs}\, 10^{(pH - pKa_{1,i})}}{1 + 10^{(pH - pKa_{1,i})}} \tag{3.11}$$

In general, we want to simulate the following behavior:

- At high pH (pH ~ 12) Cs^+ loading,
- At neutral pH (pH ~ 7) negligible or weak elution of Cs^+ from the column,
- At low pH (pH ~ 1) strong Cs^+ elution.

There are three parameters ($k_{1,Cs}$, $k_{2,Cs}$ and $pKa_{1,Cs}$) available in Eq. (3.11) to work with. Six parameters are available if the full equation for the Cs^+ separation factor shown in Eq. (3.5) is used and more if the behavior of H^+ and X^+ are also modeled. However, for this initial trial, we will limit ourselves to Eq. (3.11). If we arbitrarily choose $pKa_{1,Cs}$ = 7, at the three pH levels of interest, Eq. (3.11) becomes:

$$\text{pH} = 12 \quad \alpha_{Cs,1}(pH) = \frac{k_{1,Cs} + k_{2,Cs}\, 10^{5}}{1 + 10^{5}} = k_{1,Cs}\, 10^{-5} + k_{2,Cs} \tag{3.12a}$$

$$\text{pH} = 7 \quad \alpha_{Cs,1}(pH) = \frac{k_{1,Cs} + k_{2,Cs}10^{0}}{1+10^{0}} = \frac{k_{1,Cs} + k_{2,Cs}}{2} \tag{3.12b}$$

$$\text{pH} = 1 \quad \alpha_{Cs,1}(pH) = \frac{k_{1,Cs} + k_{2,Cs}10^{-6}}{1+10^{-6}} = k_{1,Cs} + k_{2,Cs}10^{-6} \tag{3.12c}$$

Therefore, for the model to simulate the loading phase we must choose $k_{2,Cs} = 3015.7$ and to simulate elution we must choose $k_{1,Cs}$ to be some suitably small value. For demonstration purposes, the calculations used $k_{2,Cs} = 10$ as an arbitrary small value. Then, at a neutral pH, the Cs^+ separation factor would be 1512.8 which is the average of the separation factors at high and low pH. To reduce Cs^+ elution at intermediate pH, the mass transfer resistance in the column was increased to simulate resin shrinkage.

Combining the above equations, our final model for Cs^+ loading and elution is given by the isotherm shown in Eq. (3.4) with the separation factors:

$$\alpha_{H,1} = 1$$

$$\alpha_{Cs,1} = \frac{10 + 3015.7 \times 10^{(pH-7)}}{1+10^{(pH-7)}}$$

$$\alpha_{X,1} = 1$$

Using the above isotherm formulation, a demonstration VERSE-LC calculation was performed to simulate Cs^+ loading and elution from the Small Column Ion-Exchange (SCIX) process using the SRS Tank 1 waste composition containing 1.81e-04 M Cs^+ (Smith, 2007). To avoid complications, the existing model containing a lead-lag column configuration was both loaded and eluted. The loading and elution were made as two separate VERSE-LC calculations. That is, the loading calculation was run saving a VERSE-LC output (**yio**) file that was then used to initialize the elution run. This method allowed testing elution parameters without rerunning the loading phase of the calculation.

Following column loading, an elution calculation was made in two stages:

- At time zero, the H^+ concentration was increased from 1.0e-12 to 1.0e-7 (pH = 7) to simulate column washing with a water flow of 10 gpm. This flow was maintained for 400 minutes. Since a single column bed volume is about 430 gallons, this represents washing the dual column configuration with about four total bed volumes. Note: this approach excludes the feed displacement step with dilute caustic, which was not considered necessary at this stage of model development.
- At 400 minutes, the H^+ concentration was increased from 1.0e-7 to the elution pH to simulate column elution while maintaining the flow at 10 gpm.

Results from elution calculations at pH 1, 3, 4 and 5 are shown in Figure 3.3. At low pH, the peak cesium concentration in the eluant solution occurs about 100 minutes after the pH change or after approximately one bed volume of eluant flow. The double peaks in the eluant concentration profiles are probably caused by some Cs^+ redistribution within the bed during the washing phase. Figure 3.4 shows a log plot of the Cs^+ and H^+ elution profiles at pH =1 and pH = 5. The elution curves show the correct general behavior but do not agree well with the experimental data which tends to show sharper elution peaks and greater separation between the peaks at different pH values. This isotherm necessarily predicts some degree of elution at the intermediate pH.

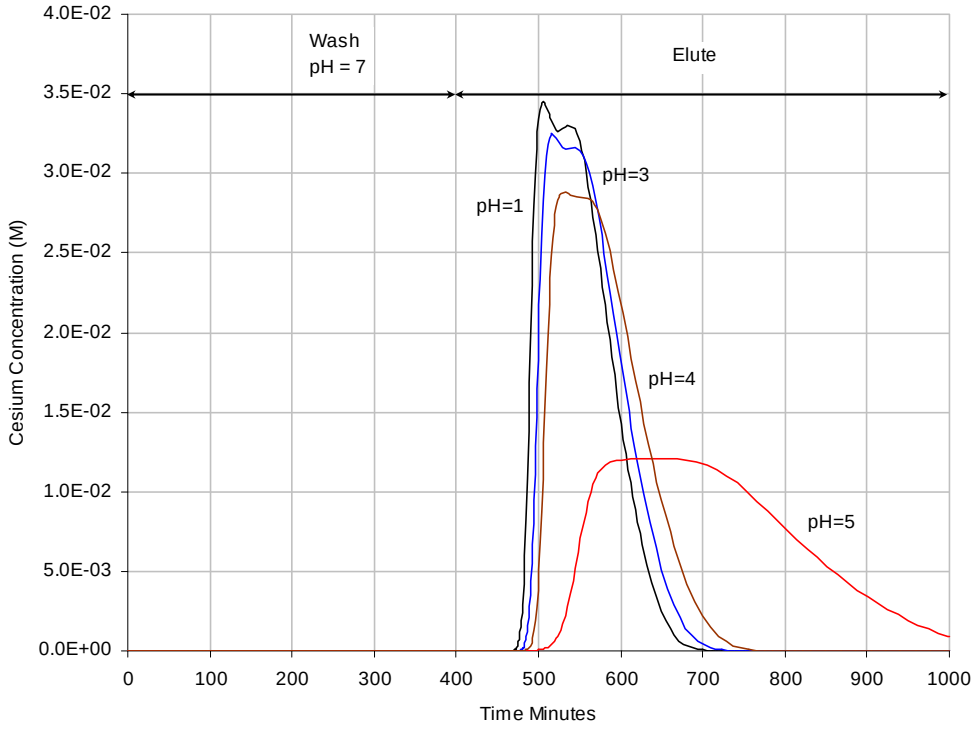

Figure 3.3 Cesium elution profiles with Separation Factor isotherm at different pH values.

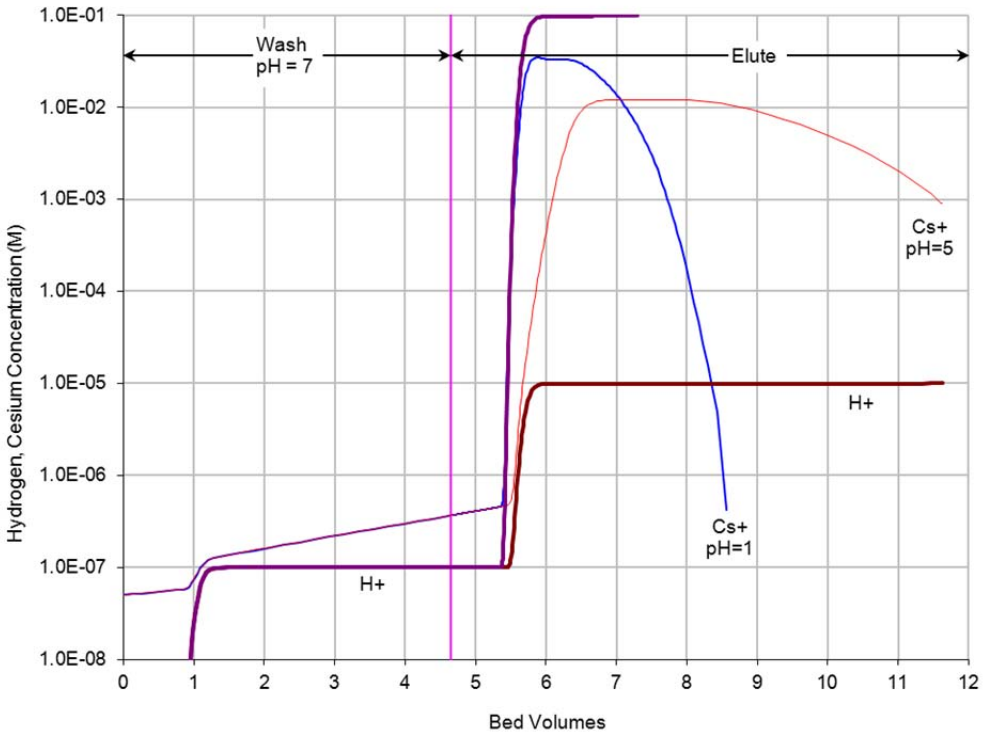

Figure 3.4 Cesium and H^+ elution profiles with Separation Factor isotherm at pH=1 and pH=5.

3.3 Mass Action Isotherm

A third approach to modeling cesium loading, displacement, and elution on sRF was tested using a four component (Cs^+, Na^+, K^+, H^+) isotherm based on the non-equilibrium mass action equation model available in VERSE-LC. This model directly uses the equations for ion-exchange and was found to be the most favorable approach. Mass action equations for the four component system are:

$$\overline{[Na^+]} + [Cs^+] \overset{K_{Cs}}{\Leftrightarrow} \overline{[Cs^+]} + [Na^+] \tag{3.13a}$$

$$\overline{[Na^+]} + [K^+] \overset{K_K}{\Leftrightarrow} \overline{[K^+]} + [Na^+] \tag{3.13b}$$

$$\overline{[Na^+]} + [H^+] \overset{K_H}{\Leftrightarrow} \overline{[H^+]} + [Na^+] \tag{3.13d}$$

In Equations (3.13a – 3.13c), the over-bar indicates species adsorbed on the ion-exchange resin while ions without the over-bar are in solution. Forward and reverse rate constants are input for each reaction. Using the non-equilibrium formulation gives more flexibility to the model and is at the same time easier for VERSE-LC to solve. If the forward and reverse reaction rates are set sufficiently large, the model will simulate equilibrium behavior. The sodium ion (Na^+) was chosen as the reference species which means that reaction rates for Cs^+, K^+ and H^+ adsorption and desorption are relative to Na^+. Using Na^+ as a reference also means that some Na^+ must be present in the system at all times.

An example calculation was performed using column data from a PNWD ion-exchange experiment (Fiskum et al., 2006) using diluted feed (DF) of actual waste from Hanford waste tank AP-101. The feed composition was:

Table 3.2 Feed composition of AP-101 diluted feed.

Cation	Molarity
Na^+	5.165
K^+	0.737
Cs^+	4.484e-5

The PNWD experiment used a lead/lag column configuration. Effluent from both the lead and lag columns were analyzed for cesium during the loading phase. Effluent from the lag column was measured during the displacement and rinsing phase. Effluent from the lead column was measured during the elution phase. Calculations using the SRNL thermodynamic model of sRF ion-exchange gave an apparent resin capacity for cesium of 0.68 mmol/g resin. These calculations were also used to obtain the values of K_{Cs} and K_K shown in Table 3.3 with K_H assumed to be 10.

Table 3.3 Equilibrium constants used in model.

Equilibrium Constant	Ion Pair	Value
K_{Cs}	Cs^+:Na^+	2.048e+4
K_K	K^+:Na^+	4.393e+1
K_H	H^+:Na^+	1.000e+1

Figures 3.5a and 3.5b show linear and log scale plots, respectively, of cesium breakthrough predictions from the lead column for AP-101 DF calculated with a single component (Cs^+) Langmuir isotherm and with the four component (Cs^+, Na^+, K^+, H^+) mass-action isotherm compared to PNWD experimental data. The calculations used the resin capacity and equilibrium constants shown above. This result demonstrated that using the mass-action isotherm with consistent parameters will reproduce results obtained with a Langmuir isotherm. Figures 3.6a and 3.6b show linear and log scale plots, respectively, of cesium breakthrough predictions from the lead column for AP-101 DF with an unmodified (i.e., the same as in Figures 3.5a and 3.5b) four component (Cs^+, Na^+, K^+, H^+) mass-action isotherm and a modified isotherm compared to experimental data. The modified mass action calculation was changed by increasing the resin capacity by a factor of 10 (6.8 mmol/g –resin) to represent the total resin capacity and also by trial and error decreasing the equilibrium constants by a factor of 67. This demonstrates that the mass action isotherm can reproduce resin loading behavior using the total resin capacity with adjusted equilibrium constants.

Figures 3.7a and 3.7b show linear and log scale plots, respectively, of the cesium distribution profiles in the lead column liquid phase after AP-101 loading and following solution displacement with 8 bed volumes (BV) of 0.1 M NaOH and water rinsing with7 BV. These calculations used the same isotherm parameters as were used for Figure 3.6a and 3.6b. The results are reasonable, showing almost complete removal of cesium from the liquid phase as the solution passes through the column. Figures 3.8a and 3.8b show linear and log scale plots, respectively, of the cesium concentration in the effluent from the lead column during the displacement and water rinse steps. These profiles were not measured experimentally. Profiles from the lag column during displacement and washing were measured but we have not simulated the lag column in this preliminary study. However, the results appear to show the expected trend.

Figures 3.9a and 3.9b show linear and log scale plots, respectively, of model predicted Na^+, K^+, H^+ and Cs^+ breakthrough from the lead column during elution following AP-101 loading. Figures 3.10a and 3.10b show linear and log scale plots, respectively, of results from a trial calculation of model predicted cesium concentrations during elution from the lead column using 0.5 M HNO_3 compared to experimental data. For elution modeling, the cesium forward reaction rate was decreased by a factor of 10 and the reverse reaction rate increased by a factor of 10. Results show qualitative agreement with the experimental data but indicated only 70% cesium recovery.

VERSE-LC includes the effect of well mixed solution volumes which typically exist at the inlet and outlet of ion-exchange columns. For example, the user can obtain the time history of the concentration exiting directly from the packed ion-exchange resin bed or the time history of the concentration exiting from a well-mixed volume at the column exit. In previous work, we have compared the column exit concentration or the concentration from the mixed volume at the column exit to experimentally measured effluent concentrations. This is not an exact comparison because the experimental concentrations typically are not measured instantaneously, but represent the average concentration in a relatively large volume of composite column effluent. Although VERSE-LC is not capable of providing a volume average concentration, the output from VERSE-LC can be collected and the volume average concentration calculated externally. This technique was implemented to give the results shown in Figures 3.9a and 3.9b. For this experiment, the mixing volume at the column exit was reported to be only 1.0 ml while the total column volume was 11 ml. As a result, there is little difference between the instantaneous column exit concentration (Column Outlet) and the concentration exiting the mixed volume (CSTR Outlet) as shown in the figures. However, the actual effluent sample volume was 15.6 ml. When the sample volume is accounted for, much better agreement between the calculated and measured results is obtained, as shown in the plot for results labels as “Samples”.

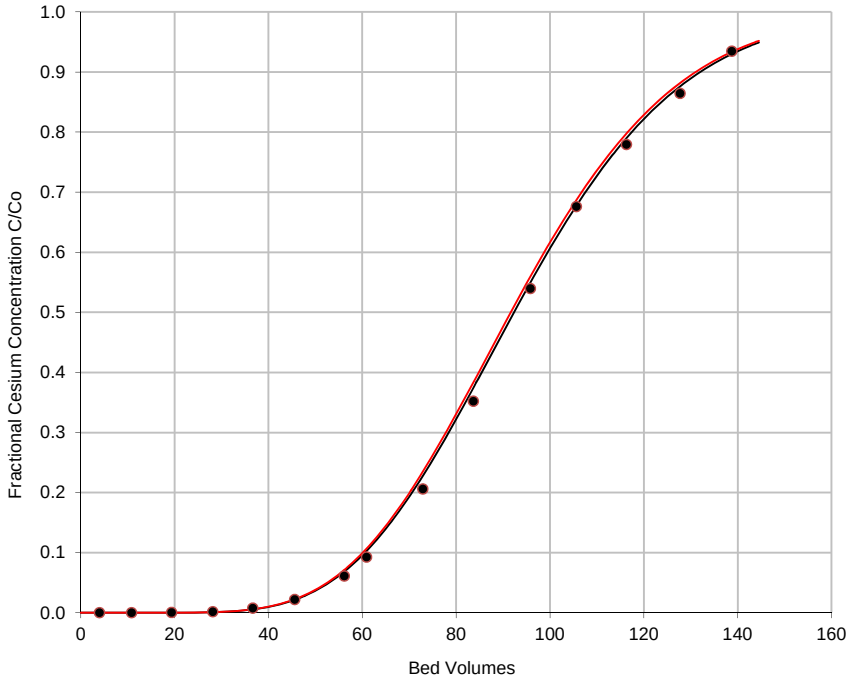

Figure 3.5a Linear scale plot of experimental data and predicted cesium breakthrough for lead column effluent during loading with AP-101 DF using single component (Cs^+) Langmuir and four component (Cs^+, Na^+, K^+, H^+) mass action isotherms.

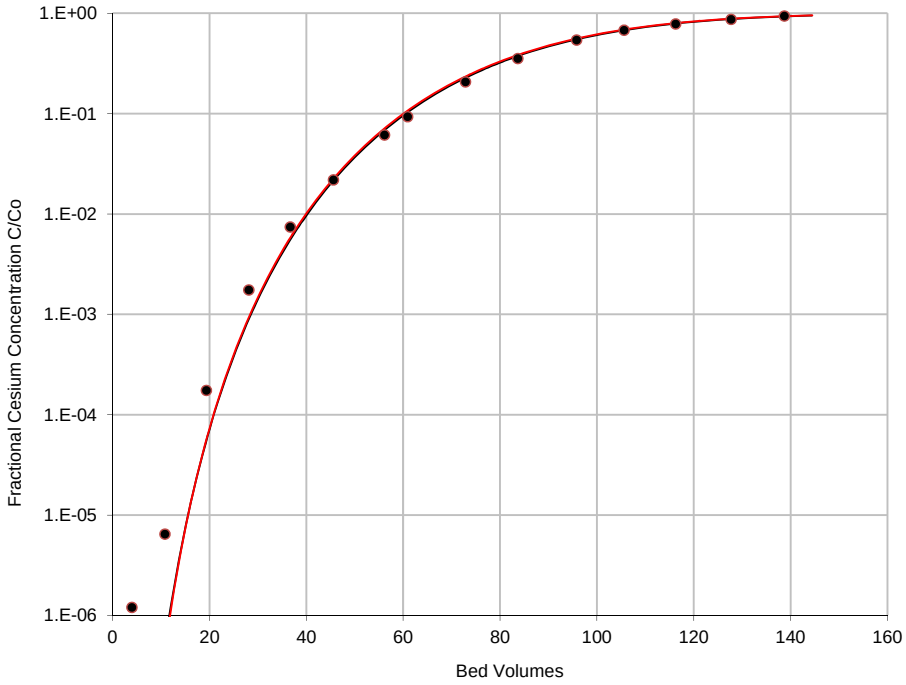

Figure 3.5b Log scale plot of experimental data and predicted cesium breakthrough from lead column effluent during loading with AP-101 DF using single component (Cs^+) Langmuir and four component (Cs^+, Na^+, K^+, H^+) mass action isotherms.

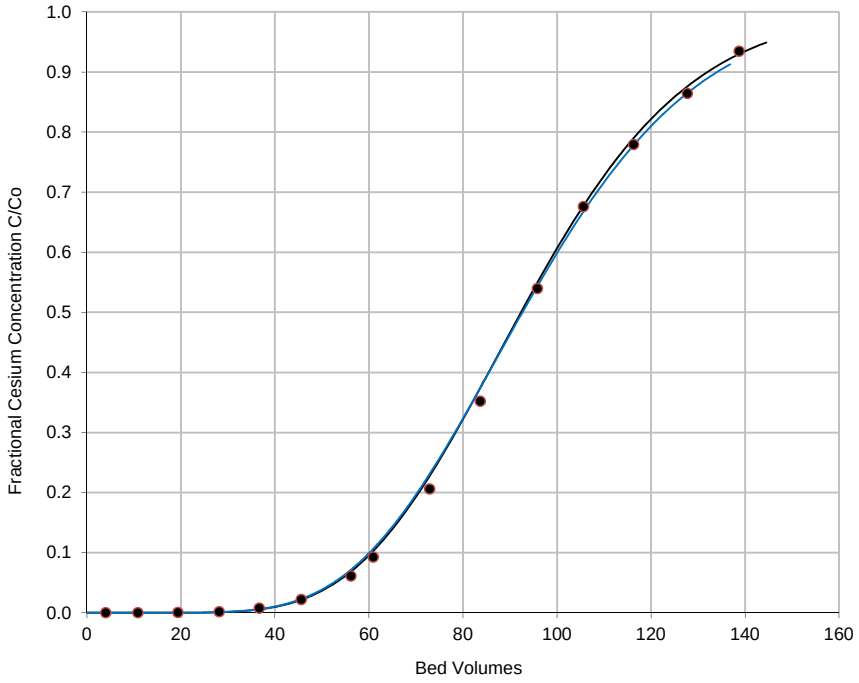

Figure 3.6a Linear scale plot of cesium breakthrough predictions for lead column effluent with AP-101 DF using four component (Cs^+, Na^+, K^+, H^+) mass action isotherms with different resin capacities compared to experimental data.

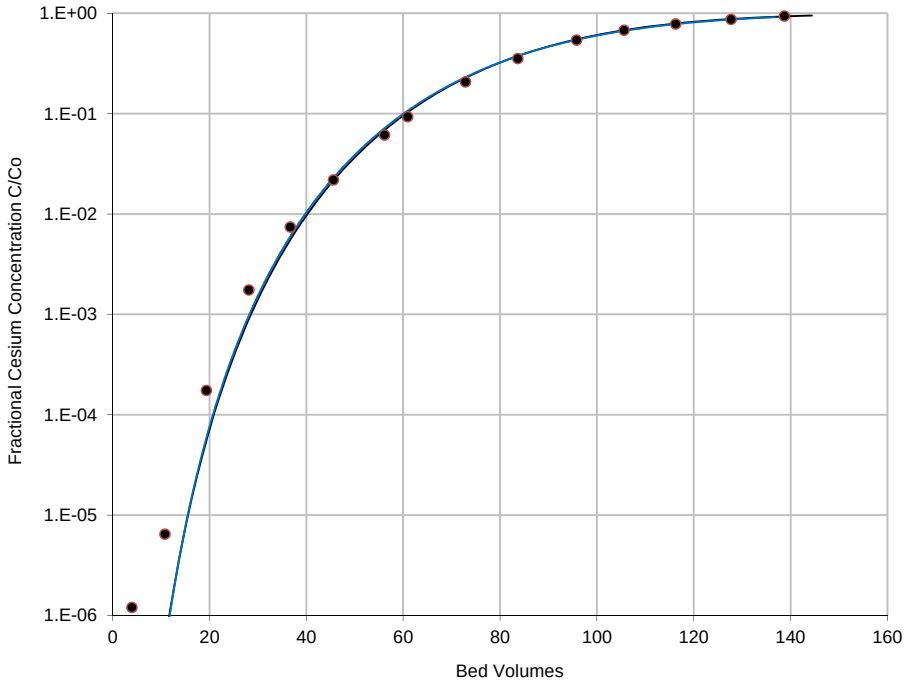

Figure 3.6b Log scale plot of cesium breakthrough predictions for lead column effluent with AP-101 DF using four component (Cs^+, Na^+, K^+, H^+) mass action isotherms with different resin capacities compared to experimental data.

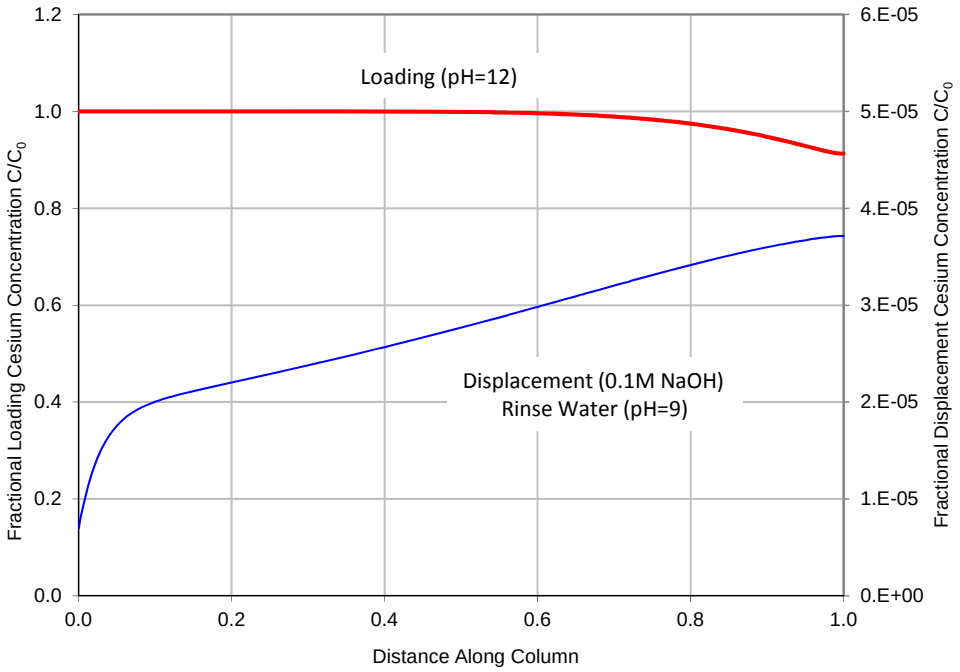

Figure 3.7a Linear scale plot of liquid phase cesium concentration profiles in lead column after AP-101 loading and following feed displacement with 0.1 M NaOH and water rinse.

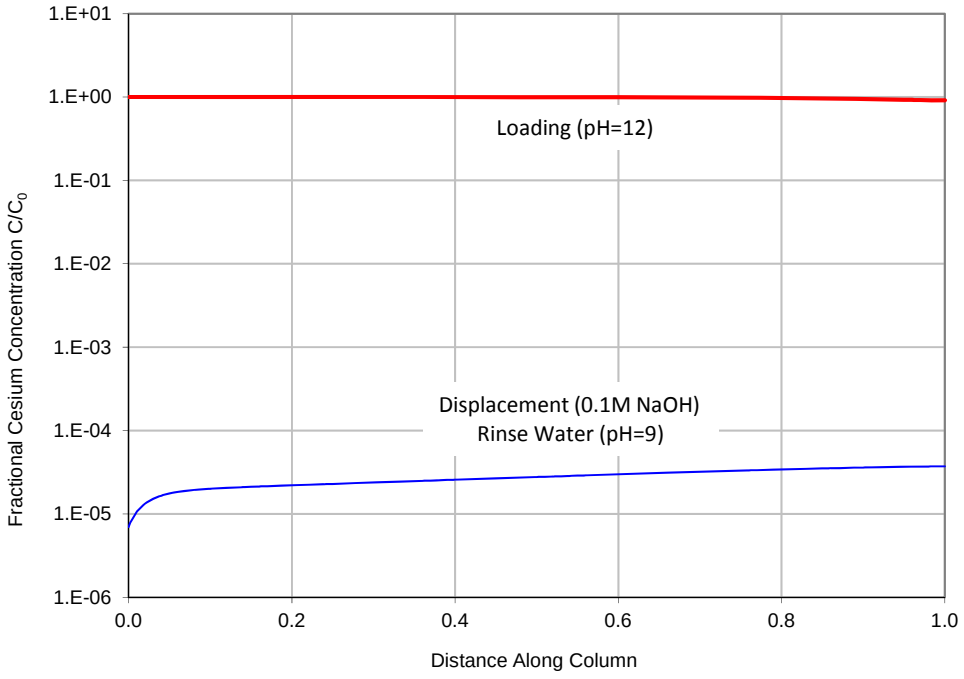

Figure 3.7b Log scale plot of liquid phase cesium concentration profiles in lead column after AP-101 loading and following feed displacement with 0.1 M NaOH and water rinse.

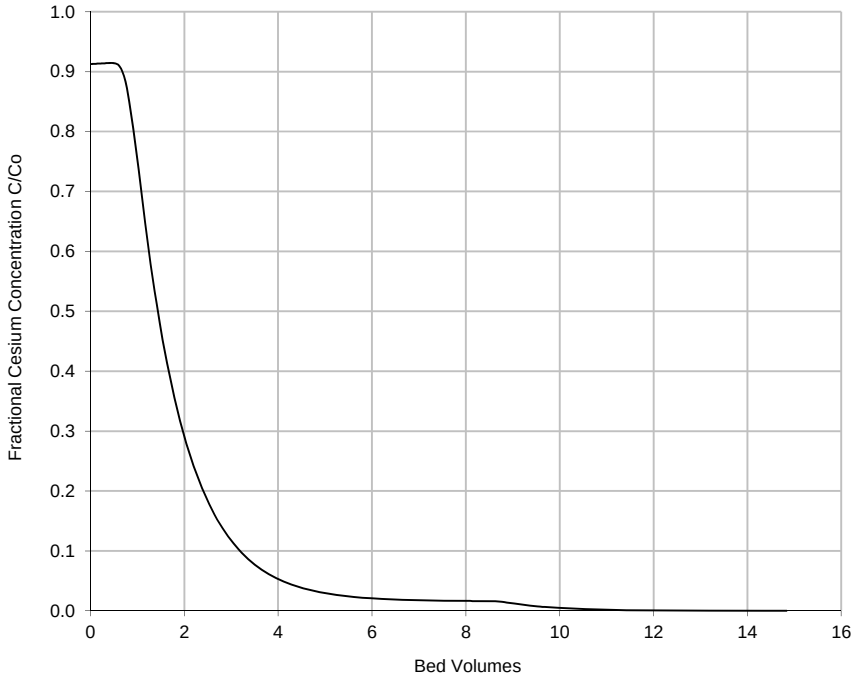

Figure 3.8a Linear scale plot of cesium concentration in effluent from lead column during displacement and water rinse steps following AP-101 loading.

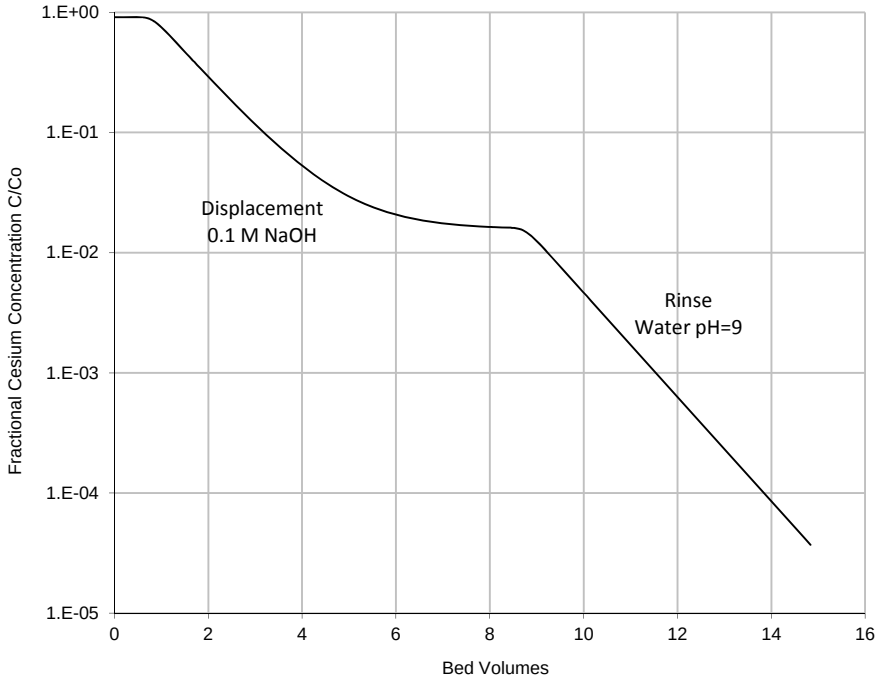

Figure 3.8b Log scale plot of cesium concentration in effluent from lead column during displacement and water rinse steps following AP-101 loading.

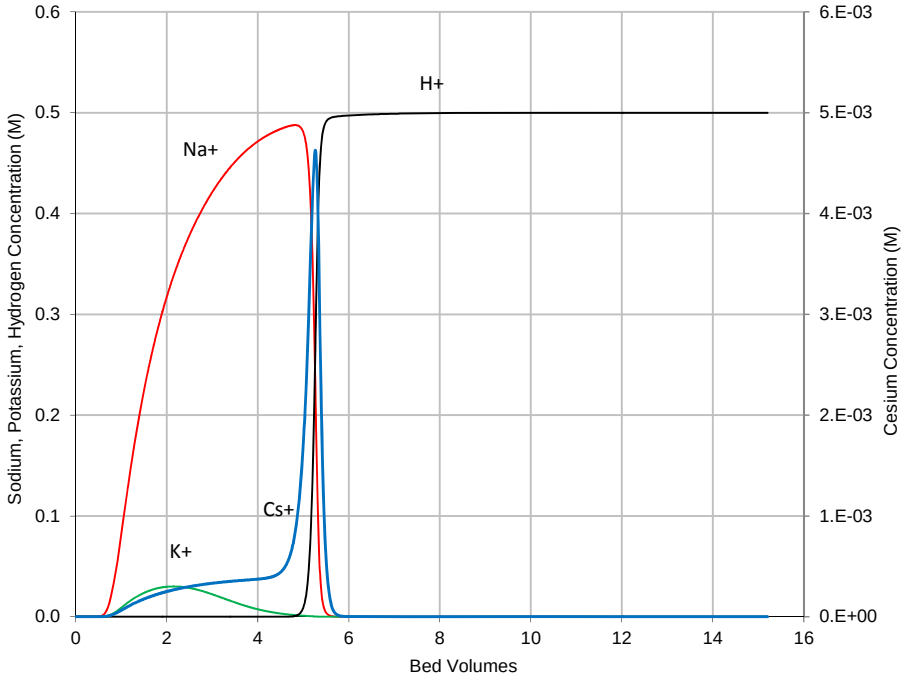

Figure 3.9a Linear scale plot of model predicted Na^+, K^+, H^+ and Cs^+ breakthrough from lead column during 0.5 M HNO_3 elution following AP-101 loading.

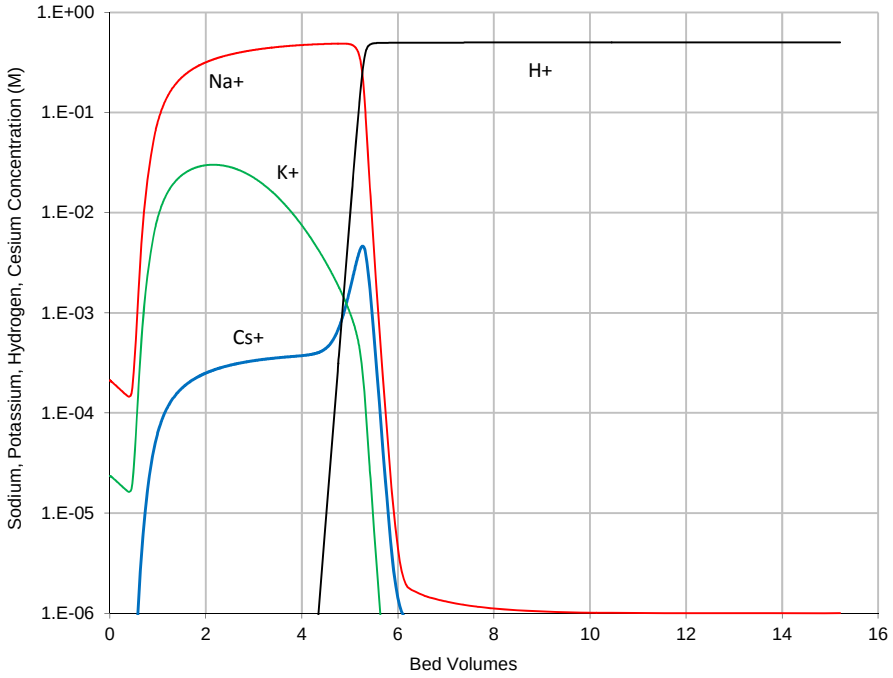

Figure 3.9b Log scale plot of model predicted Na^+, K^+, H^+ and Cs^+ breakthrough from lead column during 0.5 M HNO_3 elution following AP-101 loading.

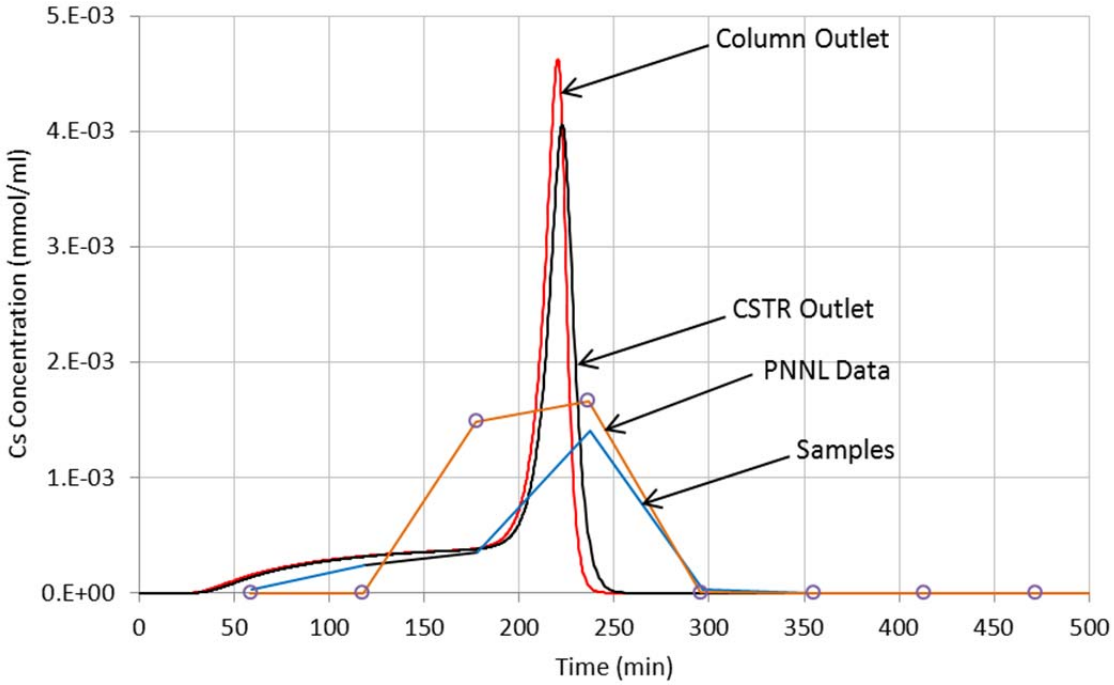

Figure 3.10a Linear scale plot of results from a trial calculation of model predicted cesium elution from lead column using 0.5 M HNO_3 compared to experimental data following AP-101 loading.

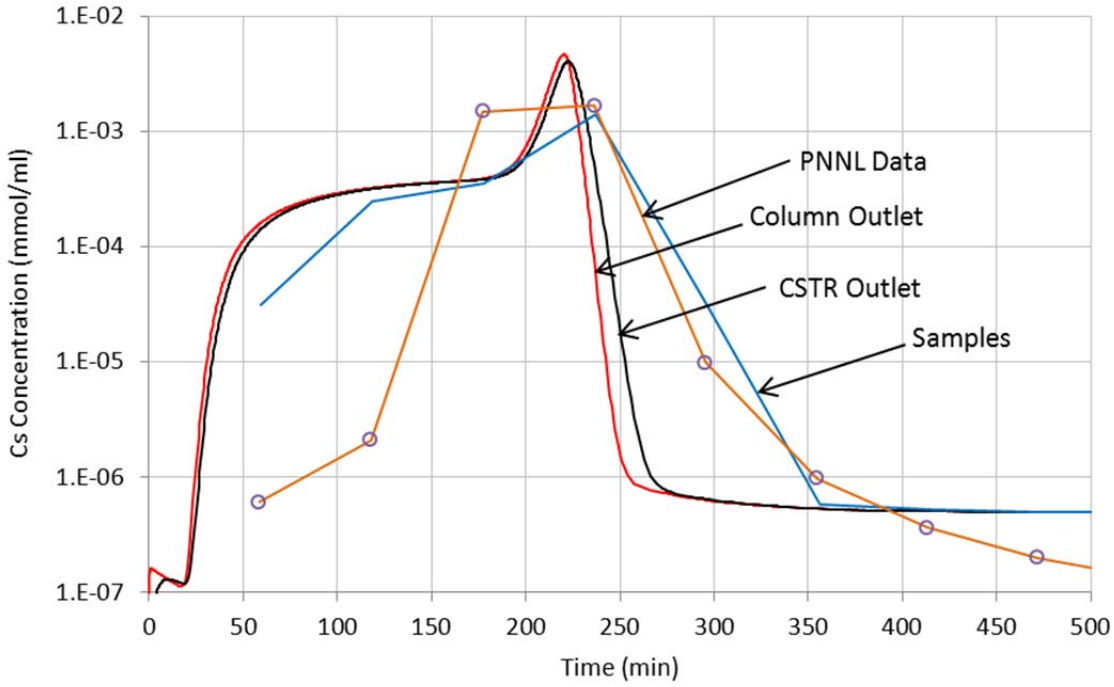

Figure 3.10b Log scale plot of results from a trial calculation of model predicted cesium elution from lead column using 0.5 M HNO_3 compared to experimental data following AP-101 loading.

3.4 Conclusions from Column Modeling Tests

Three possible methods of modeling all phases of ion-exchange column operation including loading, feed displacement and washing, and elution were investigated in the 2011 study. The three methods investigated were: 1) Multicomponent Freundlich/Langmuir isotherm, 2) pH dependent separation factor isotherm, and 3) Multicomponent mass-action isotherm. All of the isotherms were able to predict column loading behavior with reasonable accuracy. To some extent, all of the isotherms were also able to show expected aspects of column elution behavior. However, it was concluded that using the mass-action model provides the best approach to accurately capturing column performance over the complete range of operating conditions. This isotherm directly models the ion-exchange behavior of cations. As described in Section 3.0 of this report, it appears feasible to develop isotherm parameters using a thermodynamic based approach and experimental data over the complete range of column operating conditions. When this is coupled to the VERSE-LC column model it should be able to accurately predict column performance over the entire pH range from loading to elution. Also, as noted in Section 3.3, a method for calculating a model predicted effluent concentration directly comparable to experimentally measured concentrations has been developed and will be used in future studies.

Appendix A provides a list of 28 column experiments from eight different studies that potentially can be used to validate a VERSE-LC model. Not all of the available data is ideal for model validation. For example, 12 of the 28 experiments had either no or low cesium breakthrough during the loading phase. Without a full loading curve to compare the model to, it is difficult to verify the loading isotherm.

4.0 Isotherm Modeling

In this section, we provide a discussion of the approach being taken to develop a robust isotherm model that can be used for column modeling as described in Section 3.3.

4.1 Polyfunctional Ion-Exchange Resin

A brief discussion on the behavior of polyfunctional ion exchange resins is provided in Chapter 5 of Helfferich (1962). The simplest ion exchange resins are homogeneous in structure and all of their fixed ionic groups are identical in their behavior. A classic example of such a cation exchange resin is Dowex-50 (Bauman, 1946; Bauman and Eichhorn, 1947; and Bauman et al., 1948). As stated by Helfferich (1962): "For monofunctional addition polymers, especially styrene-type ion exchangers, this assumption usually holds quite well. However, it is by no means generally valid."

It was readily known that resorcinol-formaldehyde resins have two phenolic groups per ring with different dissociation constants (i.e., pKa values estimated to be approximately 9.2 and 11.3; see Hubler et al., 1995). This granular RF resin material (Bibler et al., 1990) was considered a bifunctional cation exchange resin containing only the two phenolic groups per ring.

During the initial development phase for the ion exchange process to remove cesium from Hanford waste, the SuperLig 644 resin was the primary resin of choice. SuperLig 644 was a granular resin with a high apparent capacity for cesium along with a significant volume change during the large pH shifts that occur from loading to elution conditions. Adverse hydraulic conditions during resin swelling strongly indicated that a low length-to-diameter (L/D) geometry of the columns was required. Other efforts to design a spherical resin to replace SuperLig 644 were undertaken. Spherical resins generally have lower angles of internal friction and are less likely to fragment along their edges during process cycling. Based on the earlier research on the granular RF resin, research efforts focused on the creation of a spherical resorcinol-formaldehyde version (sRF).

The creation of sRF resin follows a condensation reaction process where spherical seeds of sulfonated polymers are reacted in the presence of formaldehyde. It is reasonable to expect (even based on our "limited" knowledge of this reaction sequence) that the ionogenic acid groups formed which constitute the sRF exchange sites are a mixture of the sulfonic (SO_3H), carboxylic (COOH), and phenolic (OH) types which should be present in the resin structure primarily in the phenol-aldehyde form. The phenolic groups show up as pairs on benzene rings and are generally referred to as resorcylic (OH) groups that represent the desired and dominant number of groups present. The source of carboxylic groups is believed to result from partial decomposition of the resin during its (1) curing process at elevated temperatures and (2) aging process in the presence of oxygen and carbon dioxide (e.g., degradation by oxidation during storage). At this point in our level of understanding, it is unclear whether or not the formation of carboxylic groups results in the loss of corresponding resorcylic groups or the alteration of their electrochemical properties. The sulfonic groups come directly from the original seed material and, though small in number, their impact on isotherm behavior may be important at low pH.

Early studies of ion exchange resins by Topp and Pepper (1949) addressed polyfunctional resin behavior where a range of resins were tested through standard titration studies. At the end of their paper they state: "In applications where the pH varies only slightly, a poly-functional

material may be quite satisfactory, but where large variations in pH are encountered, e.g., in some chromatographic separations, monofunctional resins are superior in that only one set of fundamental data regarding distribution constants, rates of change, and swelling is required." For sRF we envision at least three ring types that play a potential role in its performance within the proposed range of WTP process conditions. In addition, these ring types have different numbers of ionogenic groups on them. All of which complicates our ability to adequately characterize its behavior over large pH shifts. When looking at the results from the numerous experimental studies that have been undertaken on sRF over the past approximately ten years, the above information helps in our understanding.

It is clear that over the range of pH values encountered from loading to elution sRF resin should be viewed as a polyfunctional ion exchanger. It is also likely that this resin should be viewed as having a somewhat inhomogeneous structure. As stated by Helfferich: "Many ion-exchange resins, particularly the condensation polymers, are inhomogeneous in colloidal dimensions. They consist of "islands" of high crosslinking and fixed-charge molality embedded in regions of much lower crosslinking and fixed-charge molality." We will focus our attention in this report on only the equilibrium behavior of sRF and not attempt to address its mass transport aspects at this time.

As stated by Helfferich (1962), for polyfunctional resins each ionogenic group will behave according to its general behavior; however, the different types of groups may well counteract one another. Specifically he states: "The behavior of a polyfunctional resin is similar to that of a mixture of different monofunctional resins containing, in total, the same amounts of the various ionogenic groups." One example of this for a bifunctional resin is provided by Cornaz and Deuel (1956) who tested Lewatit H-236, a bifunctional resin containing sulfonic and carboxylic acid groups. For comparison purposes they also tested a mixture of the two resins with an equal ratio of groups: (1) Dowex 50 (monofunctional resin with sulfonic groups) and (2) Amberlite IRC-50 (monofunctional resin with carboxylic groups). Figure 4.1 below shows their results in the form of equivalent ionic fractions within the aqueous phase versus resin phase.

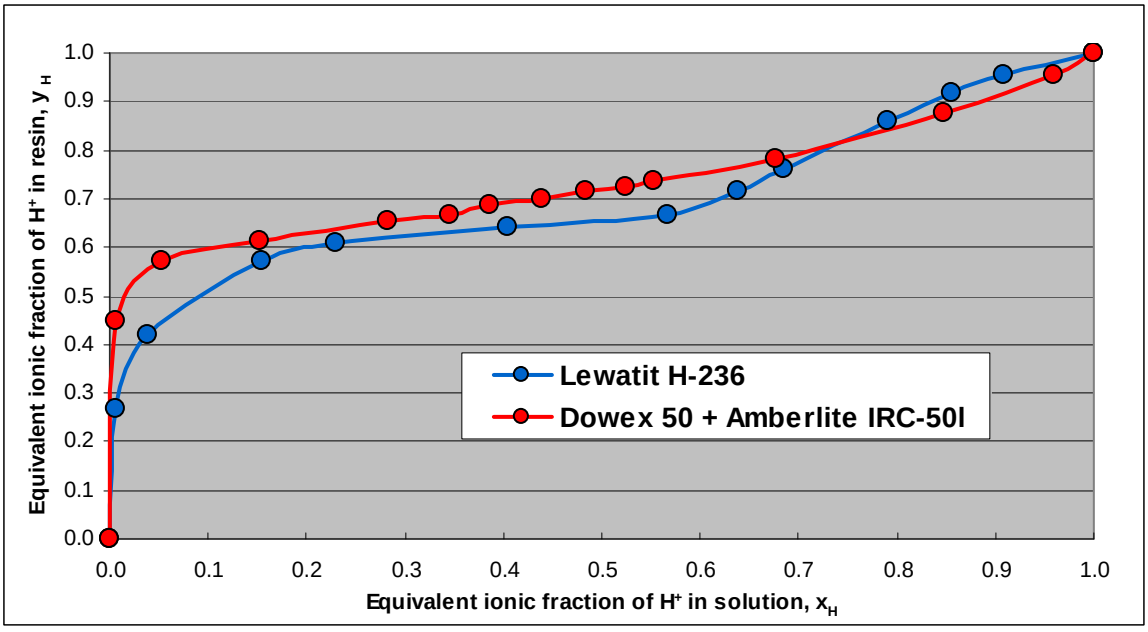

Figure 4.1 Comparison of isotherms for a bifunctional cation exchange resin and a mixture of monofunctional resins containing each ionogenic group type.

As stated by Helffrich (1962) and Cornaz and Deuel (1956) the resin mixture (shown in red) isotherm is strictly an additive result of the individual isotherms. The selectivity differences between this mixture resin and the bifunctional resin (shown in blue) is attributed to electrochemical interactions within the bifunctional ionogenic groups. However, it is still useful to point out that the mixture resin approach shown does a fairly reasonable job in estimating the behavior of the bifunctional resin. An even better approximation can be achieved if the pK_a values of the two ionogenic groups (i.e., sulfonic and carboxylic acid groups) are adjusted to account for their apparent environmental shifts.

It is the success of this sort of effort that have lead us to consider for sRF an "Ideal Mixture Model" to be defined in more detail in the following sections. A simple, and analytic, deprotonation model was developed to test the mixture approach as outlined above. As to be shown in later sections, the results of this simple deprotonation model, along with information from the open literature, confirms our conceptual model of sRF.

The following is a brief outline of the various key steps being taken to develop a robust isotherm model for sRF resins:

- Development and testing of a multi-site deprotonation model (Appendix B).
- Development and testing of a simple analytical isotherm model for the purposes of checking out concepts and for code verification (Appendix C).
- Development and testing of a simple numerical isotherm model for scoping studies (Appendix D). This model will not attempt to address (1) non-idealities within either phase (e.g., activity coefficients of ionic species within aqueous phase), (2) Donnan invasion of neutral species, or (3) osmotic pressure effects on selectivity.

With successful completion of the above development steps, the final step becomes:

- Development and testing of the numerical isotherm model (future activity). Here the various omitted features listed above for the simple numerical model will be addressed. Some of these items already reside within the existing sRF isotherm model CERMOD (Aleman and Hamm, 2007).

Given the expected lifetime of operations of the WTP, it is envisioned that future batch-to-batch variability will exist between sRF resins employed. The final model should accommodate this variability through input parameters such as the resin batch's scientific weight capacity, ring types present, ring type number fractions, and pK_a values of ionogenic groups.

4.2 Ideal Mixture Model

Based on the motivation provided in the previous section, an "Ideal Mixture Model" for predicting the isotherm behavior of sRF has been developed. The goal is the prediction of isotherm behavior over the entire expected pH range for sRF ion exchange (i.e., pH from 0 to 14).

The polyfunctional ion exchanger for sRF is assumed to be made up of the following three ionogenic ring types:

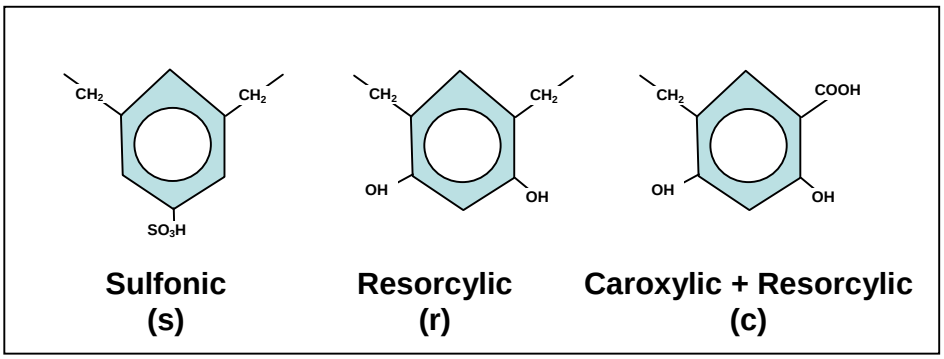

Figure 4.2 The three ring types considered in the Ideal Mixture Model of sRF.

As Figure 4.2 indicates, the three ring types have varying numbers of ionizable sites:

- Nuclear sulfonic ring type (s) has one site per ring;
- Resorcylic ring type (s) has two sites per ring; and
- Carboxylic plus resorcylic ring type (c) has three sites per ring.

Note that a ring type with just a carboxylic group(s) is not being considered here but could easily be included later. The meta arrangement of phenolic groups on the resorcinol ring is believed to be the dominant structure (Fondeur et al., 2006).

We shall assume that each ring group's electrochemical properties (i.e., expressed by their dissociation constants, pK_a values) are unaltered by conditions changing on neighboring ring groups (i.e., an ideal mixture of ring groups within a solid resin phase). However, within a ring group its local sites are impacted by the state of its neighboring sites as reflected by the potential to have different pK_a values within a ring (i.e., a multi-site model).

In reality there are many more ring types than just the three chosen ones listed above. For example, there are probably two other potential geometries for the (r)-ring type where the configuration (locations) of phenolic groups and CH_2 linkages differ (Fondeur et al., 2006). The basic approach taken here can easily accommodate these other ring types once such types are determined to be of importance.

This assumed independence of ring group behavior allows us the option to create ion exchange isotherms for each of the three ring types independently (i.e., a significantly less complicated numerical problem to solve). The isotherm behavior of the actual sRF resin then becomes a simple mixture of these group type isotherms computed by number weighting of the amounts of each group present. The impact on sRF behavior due to process changes and process exposures then becomes addressable through varying these number fractions directly. For example, carboxylic groups are believed to be generated on the cross-linkage of the original (r)-rings when resin degradation is taking place say during chemical attack from the presence of O_2 and/or CO_2. Here (r)-rings are being converted into (c)-rings where the total number of functional rings remains constant (however, the total number of functioning sites increases). This effect is simply handled by alterations in the specified total scientific weight capacity and the number fraction of ring types present.

The conceptual model of this "ideal" mixture can be mathematically viewed as separate resins each consisting only of one ring type. When at chemical equilibrium at a specified temperature

(i.e., an isotherm) each of these ring types are in equilibrium with the same aqueous phase solution containing the counter-ions of interest. This separation of the ring types into separate resins in contact with one common reservoir of aqueous solution is illustrated as shown in Figure 4.3. Note that the impact of co-ions within the aqueous phase is not being addressed within the simple numerical model being presented in this report. The co-ion effects must be addressed in the more complicated (future) model since expected WTP aqueous solutions will contain significant amounts contributing to Donnan invasion and non-idealities.

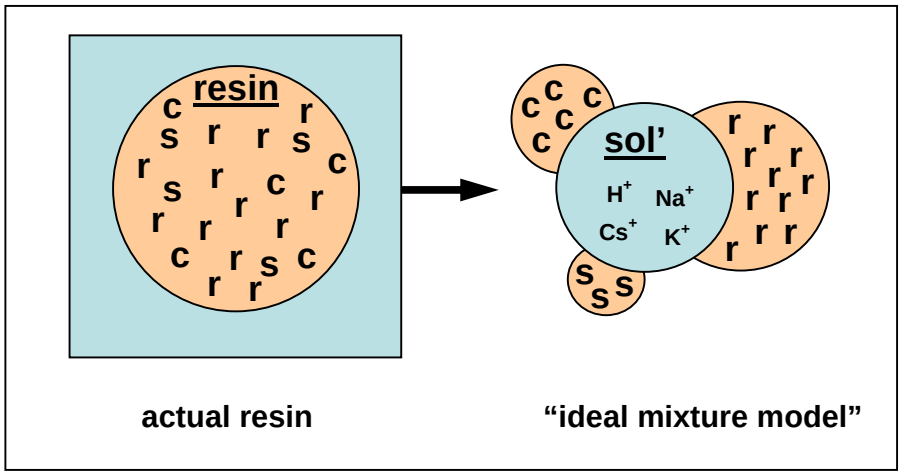

Figure 4.3 Illustration of basic concept behind the Ideal Mixture Model of sRF.

At equilibrium the liquid-phase solution is in chemical-equilibrium with each ring group present. The sequence of deprotonation of a multi-site ring group is assumed to be unaffected by its environment. Deprotonation is assumed to be based entirely on the dissociated hydrogen ion within the resin phase. Here the dissociated hydrogen ion within the resin phase is assumed to be constant throughout all the resin types present. The actual amounts of the various ring types must be supplied as input, along with the resins scientific weight capacity, but this defines the overall behavior of the sRF isotherm (i.e., "the mixture isotherm").

In the prior numerical isotherm model for sRF, contained within the Fortran code named CERMOD (Aleman and Hamm, 2007), each computed equilibrium point along an isotherm was determined by a "numerical batch contact" approach. To simplify the numerics associated with our simple numerical model represented in this report, we assumed the aqueous phase to be infinitely large (i.e., a very large phase ratio present). Thus, the specified aqueous phase concentrations are fixed at their inputted values.

The details of the simple numerical model employing the above ideal mixture concept are provided in Appendix D. Results using this model for comparison with some open literature data are shown in a later section of this report.

4.3 Titration Curves

As stated by Gregor and Bregman (1948), perhaps the best method to determine the numbers and kinds of exchange groups making up a resin is through experimental titration studies. A direct titration of the resin with a strong base in the absence and then presence of neutral electrolyte is recommended. The net effect of the neutral electrolyte (i.e., neutral salt containing the counter-ion(s) of interest) is the flushing out of the dissociated hydrogen ion from the resin phase. The

optimum degree of neutral salt present is resin dependent and at some upper concentration level invasion by the neutral electrolyte species is expected to become significant. Electrostatic (Donnan) exclusion by an ion exchanger is most effective at low electrolyte concentration levels. At increasingly higher concentration levels a breakthrough of the Donnan potential occurs. For typical WTP aqueous solutions the co-ion concentrations will most likely be high enough to expect modest amounts of sorbed electrolytes.

Numerous titration studies on strong and weak monofunctional cation exchangers are available for review within the open literature. Within this large body of work good experimental practices and guidelines are provided. Also, though more limited, are available titration studies of polyfunctional cation exchangers.

One particularly useful and pertinent titration study warrants our attention within this modeling effort. The titration study performed by Topp and Pepper (1949) looks at a variety of cation exchangers that are monofunctional as well as polyfunctional in nature. They looked at exchangers with different ionogenic groups present. Different combinations of sulfonic, carboxylic, phenolic, and resorcylic types were considered. In fact, resin types that are somewhat similar to the ones of interest to us were studied. One bifunctional exchanger studied referred to as "resorcylic-acid-formaldehyde" resin contained as ionizable groups: carboxylic COOH and resorcylic OH groups. The titration of this resin for the uptake of potassium is shown in Figure 4.4.

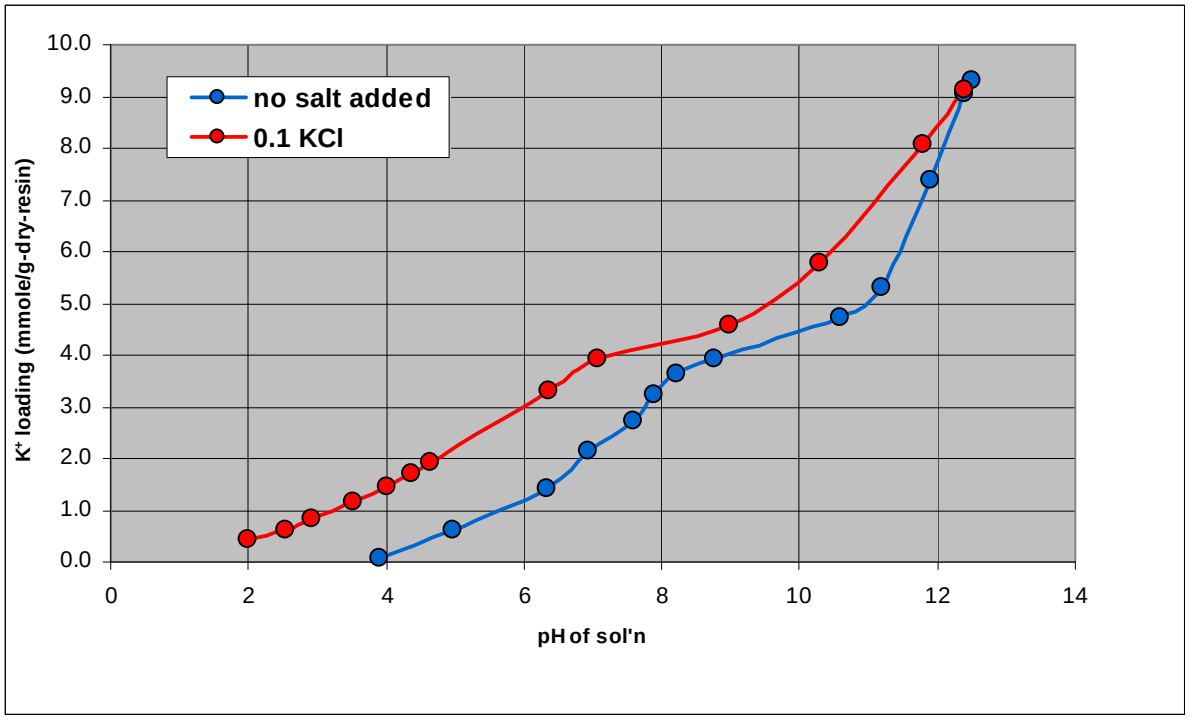

Figure 4.4 Potassium uptake of resorcylic-acid-formaldehyde resin in the absence and presence of KCl (data by Topp and Pepper [1949]).

The curves within Figure 4.4 shown the typical behavior of a weak acid resin; however, the noticeable hump in the titration curves from pH of 6 to 10 corresponds to the presence of the carboxylic groups. By knowing the functional groups present within the resin, the shapes of these curves becomes much more understandable.

The impact on the titration curve starting from the monofunctional RF resin (i.e., only resorcylic groups present), then adding carboxylic functioning groups, and then adding sulfonic functioning groups can be seen in Figure 4.5 (data taken from Topp and Pepper, 1949).

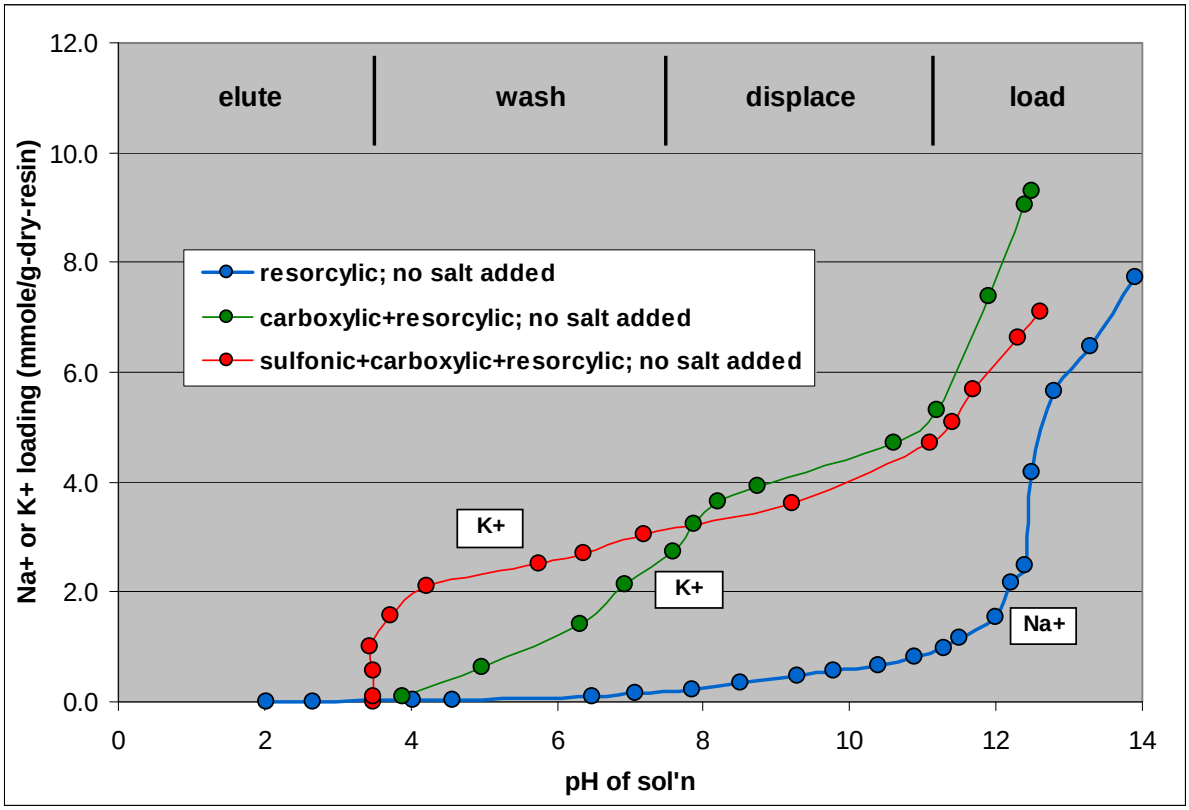

Figure 4.5 Sodium and potassium uptake of resorcylic-acid-formaldehyde resin and modified resin containing other ionogenic groups in the absence of NaCl and KCl (data by Topp and Pepper [1949]).

Overlooking the fact that selectivity for sodium versus potassium will be different for these various resins tested, the basic shapes of these titration curves clearly show the existence of the stated ionogenic groups. The nuclear sulfonic group is a strong acid group whose pK_a values range from 0-1, while the carboxylic and resorcylic groups are weak acid groups whose pK_a values range from 5-7 and from 9-12, respectively.

The ion exchange column process for WTP is cyclic in nature with the following key process steps defining one cycle:

- Loading (resin uptake of counter-ions such as Cs from ~5 M Na waste stream)
- Displacement (aqueous solution displaced with 0.1 M NaOH)
- Washing (resin washed with DI water)
- Elution (Cs displaced from column and resin converted back to H-form using ~0.5 M HNO_3)
- Regeneration (resin converted back towards its Na-form using ~0.25 M NaOH)

The typical pH ranges that the sRF resin will experience during these steps are highlighted in Figure 4.5. The isotherm behavior of the resin at the very high pH range during the loading phase should be dominated by the resorcylic groups, while at the very low pH range during the elution phase it should be dominated by the sulfonic groups. This statement is based on the assumptions that:

- At loading pH conditions all of the ionogenic groups are active but the dominant amounts of available sites are of the resorcylic group type; and
- At elution pH conditions only the sulfonic group sites are active.

As stated by Gregor and Bregman (1948): "Investigations of the resinous ion exchange process are possible only on an empirical level without a knowledge of the physio-chemical properties of the resins themselves." By knowing the numbers and kinds of exchange groups making up a resin, we can devise a model that should reasonably predict its isotherm behavior over an extended pH range. This is the premise that we are working under in the development of a robust isotherm model for sRF over its entire planned pH operating range. In the next few sections we will discuss various modeling steps taken along this route.

4.4 Simple Deprotonation Model

As stated by Baumann and Argersinger (1956): "When a particle of cation-exchange resin is placed in a solution of electrolyte whose cation is different from that in the resin, three processes are known to occur: first, equivalent cation exchange takes place until equilibrium is reached; second, water is taken up by the resin; and third, some electrolyte, in addition to that which is exchanged, is taken out of the external solution and remains associated with the resin particle. Of the processes mentioned, the cation exchange itself has been of primary interest." To date these statements also hold true for sRF resin. In this report focus is also on the cation exchange process. In the cation exchange process two basic steps are occurring:

(1) A deprotonation process is occurring within the resin phase proper where dissociated hydrogen ions are present; and

(2) Cation exchange with counter-ions held within the aqueous phase takes place.

In this section, we focus on the first of these two steps.

Surprisingly, the basic observed behavior of the sRF titration curve can be explained through the results of a "simple" multi-site polyfunctional deprotonation model. The term "simple" here refers to the various simplifying assumptions being made (to be delineated below with details provided in Appendix B) which restricts its quantitative use. This simple model was not intended for predicting cationic exchange isotherms, rather its primary purpose was to assist us in formulating a better high-level understanding as to the key features that are present over the wide pH range of intended operations (i.e., pH~ 12-14 during loading conditions down to pH~ 0-1 during elution conditions).

Note that, not disregarding these stated limitations, this simple model provided us insight and a degree of confirmation as to how sRF should be viewed conceptually. From this conceptual viewpoint more quantitative models can be constructed and better experimental focus be achieved. To illustrate the application of the conceptual view, a simple but more quantitative isotherm model is provided. Both the conceptual view and isotherm models are supported by open literature dating as far back as the 1940's. Several key references are discussed during the process of describing our current understanding of sRF behavior.

A discussion of a single-site deprotonation model is given by Helfferich (1962; Chapter 4-4 on pages 84-90) where "apparent" pK_a values are defined. An extension of this single-site model to a multi-site deprotonation model is provided by Aleman and Hamm (2007). This multi-site model was employed within the Fortran based CERMOD code used to compute monovalent cation exchange on SuperLig 644 and sRF resins.

In Appendix B the equations associated with the 1-site, 2-site, and 3-site deprotonation models required to estimate the mixture behavior of sRF are given. Also in Appendix B are the equations required to compute the ideal mixture model.

For confirmation purposes scoping titration curves for sRF (batch 5E-370/641) were performed by Nash and Polite (2011). These tests were performed starting within the H-form (low pH~2 initially achieved by addition of HNO_3) and successively stepping up in solution pH by the addition of a strong base (i.e., NaOH). Three separate series of tests were performed where the pH was increased up to ~10. Prior data (Nash and Isom, 2010 and Birdwell et al., 2010) for sRF (batch 5E-370/641) for sodium uptake at varying high pH conditions (i.e., pH~10-14) were also included in our assessment.

Table 4.1 below lists some of the key input parameter settings considered in estimating the individual ring type deprotonation behavior and then their mixture behavior. The pK_a values provided are representative values taken directly out of available open literature. No attempt was made to alter/adjust these apparent pK_a values. For example, the same pK_a values for the phenolic groups on the resorcylic ring and the isolated carboxylic group were employed on the carboxylic+resorcylic rings. The % ring fractions listed are numbers adjusted to match the sodium uptake values given by the data (i.e., no carboxylic only ring type were considered here).

Table 4.1 Parameter settings[a] employed in the simple deprotonation model to estimate sodium uptake over a wide pH range for sRF resin.

Ionogenic Group(s)	Sulfonic	Carboxylic	Resorcylic	Carboxylic + Resorcylic
Parameters				
Sites per ring	1	1	2	3
pKa1	1.0	6.5	9.2	6.5
pKa2	---	---	11.3	9.2
pKa3	---	---	---	11.3
% Ring fraction	0.25	0.0	11.0	88.75

[a] The pKa values are representative values taken from the open literature. The ring fractions were adjusted to provide a reasonable fit to the available sodium uptake data.

A comparison between the sodium uptake data versus the simple deprotonation models is provided in Figure 4.6. The three individual ring types are plotted as dashed lines indicating each level of contribution to the total resin sodium uptake shown as the solid blue line. Given the scoping nature of the titration data and the degree of assumption being made in this simple deprotonation model, the comparison is impressive. The fitted ring fraction values also seem plausible:

- 0.25% sulfonic rings appear to be somewhat consistent with the known mass fraction of sulfur present in the form of polymerization seed material.

- 11.0% resorcinol-formaldehyde rings with a carboxylic group added may appear high but is believed to be real given the age of this resin batch and the fact that these scoping titration studies were performed with exposure to the atmosphere during the NaOH addition steps.
- The remaining 88.75% is resorcinol-formaldehyde rings since no additional information is available to indicate the possibility of other group types.

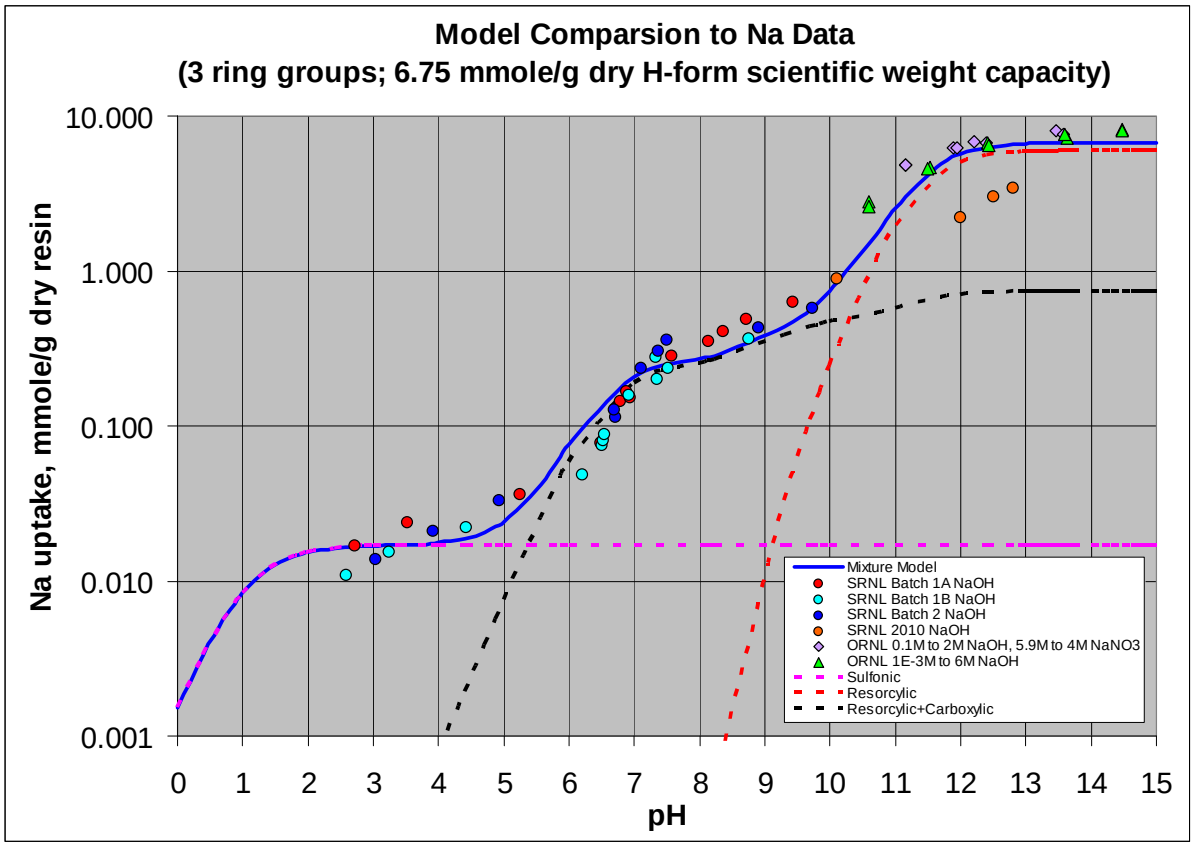

Figure 4.6 Comparison of sodium uptake data to a simple deprotonation model for the spherical resorcinol-formaldehyde resin (sRF batch 5E-370/641).

Note that the total scientific weight capacity was assumed to be equal to 6.75 mmole/g of dry resin in H-form. This particular value has been used in a variety of prior analyses for this batch (5E-370/641) of sRF. The results shown in Figure 4.6 strongly suggest (and perhaps confirm) that sRF is a polyfunctional cation exchanger whose dominant ionogenic groups are made up of sulfonic, carboxylic, and resorcylic groups.

4.5 Simple Analytical Isotherm Model

In this section we discuss a simple analytical isotherm model that was originally developed by Hale and Reichenberg (1949). Their model consists of the following three basic elements:

(1) A resin phase single-site deprotonation equation;

(2) A resin to solution phase mass action equation for one counter-ion; and

(3) An electro-neutrality balance on the resin phase.

The above model is analytic and the model along with its derivation is provided in Appendix C. This model is limited to monofunctional exchangers where only one counter-ion is being addressed.

Hale and Reichenberg (1949) looked at the H-Na equilibrium performance of two well defined monofunctional resins of their time:

- A sulfonated cross-linked polystyrene resin (SO_3H group).
- A cross-linked polymethacrylic acid resin (COOH group).

The independent variable within this model is:

$$x = \frac{[Na^+]}{[H^+]} \tag{4.1}$$

Figure 4.7 shows the predictions they made with their model (see Eq. [C-17]) versus their sodium uptake data for both resins over a wide range in x values. The batch contact tests also included a range of neutral electrolyte being present (i.e., NaCl).

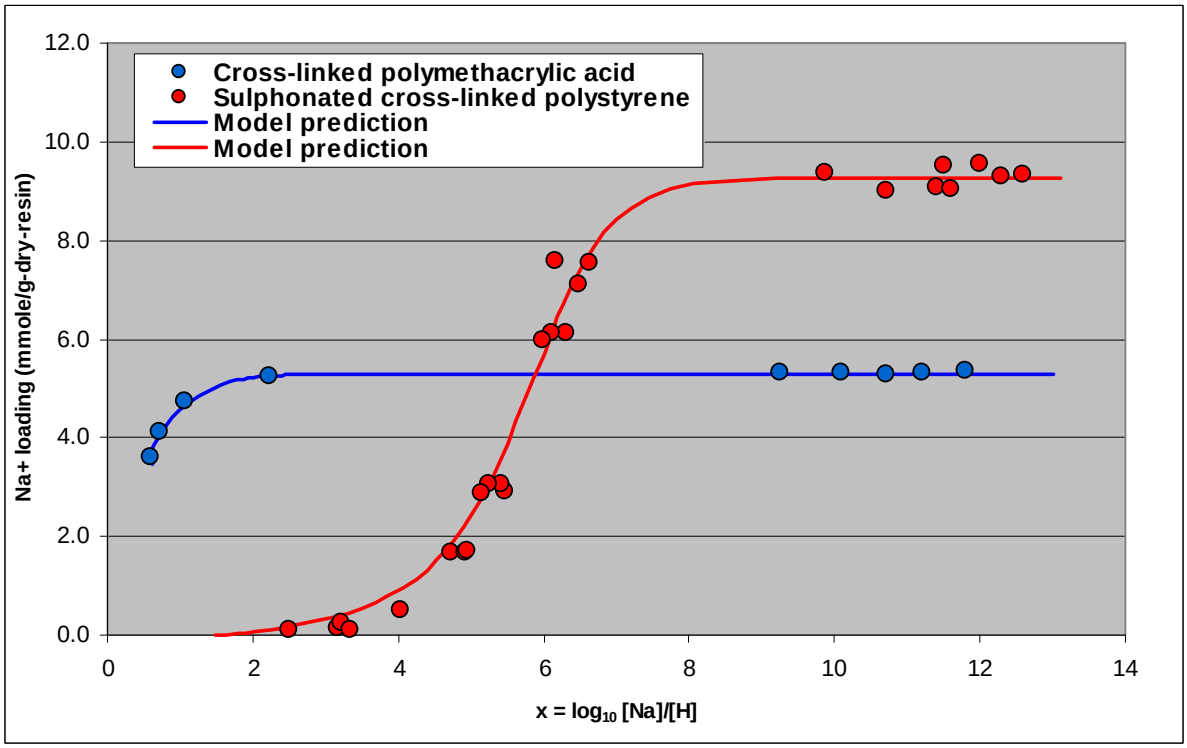

Figure 4.7 Comparison of simple analytical isotherm model to two monofunctional resins by Hale and Reichenberg (1949).

See their paper for details with regard to their tests and calculations. As Figure 4.7 illustrates, the use of the three basic elements mentioned above yielded reasonable estimates of the sodium uptake over a broad range of conditions. These results support the notion that these three elements should play a critical role within any robust isotherm model.

4.6 Simple Numerical Isotherm Model

In the above section, a simple analytic isotherm model was demonstrated to be reasonably successful under certain limiting conditions. Unfortunately, as soon as we begin to eliminate some of these limitations we immediately have an equation set that no longer can be solved analytically. Since our ultimate goal is to update the CERMOD code (Aleman and Hamm, 2007) with a robust isotherm model, the numerical model discussed within this section was written in Fortran and follows many of the conventions already employed within CERMOD.

Model limitations can be reduced by:

- Adding more counter-ions into the aqueous phase (e.g., H^+, Na^+, K^+, Cs^+);
- Adding multi-sites on a given ring type (e.g., resorcylic OH groups);
- Adding multiple ring types (e.g., sulfonic and carboxylic ring groups);
- Adding sorbed neutral species by Donnan invasion (e.g., NaCl, NaNO3, KNO3, …);
- Including non-idealities associated with ionic species in the aqueous phase (e.g., Pitzer's equation for electrolyte activity coefficients);
- Including non-idealities associated with species within the resin phase (e.g., Wilson's equation for activity coefficients); and
- Including the osmotic (swelling) pressure effect on selectivity coefficients.

The simple numerical model developed and tested within this report includes items from the first three bullets above. Appendix D provides the details associated with this model. Here only some of the results created in its development are shown.

4.6.1 Monofunctional Resins

Our first assessment of the simple numerical model was the prediction of the behavior of the two monofunctional resin data of Hale and Reichenberg (1949). Note that similar test data was also provided by Topp and Pepper (1949) for these two resins. These resins were considered to be baseline resins by both sets of authors. The preparation of these resins for batch contact titration testing was to convert the resins initially into their H-form. The resins were cycled between their Na-form and H-form to wash out impurities and to better establish a reproducible result. At the end of cycling the resins were washed until their effluents were free from chloride ion and had a pH under ~4.

For the strong acid resin (i.e., monofunctional sulfonated cross-linked polystyrene resin), its sodium uptake with and without the presence of the neutral salt NaCl is shown in Figure 4.8. As expected the sulfonic groups behave as strong acid groups (i.e., apparent pK_a values <1) and when sufficient amounts of counter-ions are presence within the aqueous phase, the total scientific weight capacity of groups become ionized at low pH conditions. At low counter-ion concentrations within the aqueous phase, large amounts of dissociated hydrogen remains contained within the resin due to Donnan equilibrium forces. The predictions using the simple numerical model are also shown and agree with the data reasonably well considering the various simplifying assumptions involved. Only one ring type is present and it contains one ionogenic group (i.e., a sulfonic group). A pK_a value of 0.0 was employed, along with a fixed value for the Na-H selectivity coefficient of 1.0 (i.e., equal selectivity for Na^+ and H^+ was assumed for trial purposes).

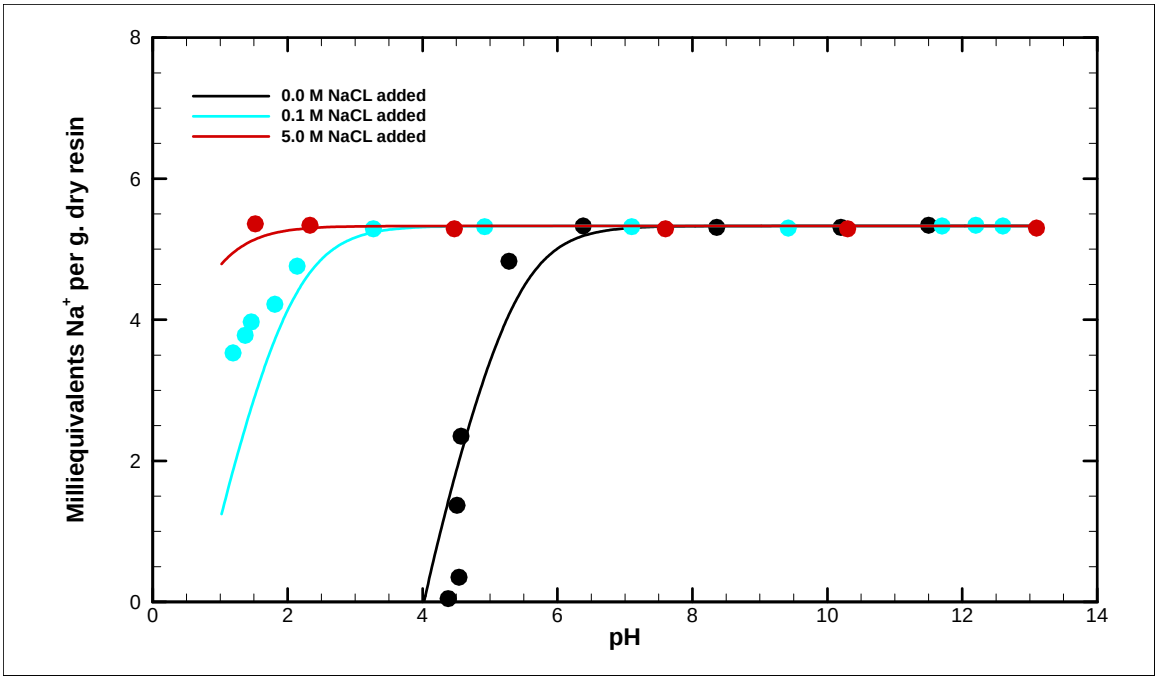

Figure 4.8 Comparison of simple numerical isotherm model to sulfonated cross-linked polystyrene resin data taken by Hale and Reichenberg (1949).

For the weak acid resin (i.e., cross-linked polymethacrylic resin), its sodium uptake with and without the presence of a neutral salt (i.e., NaCl) is shown in Figure 4.9. As expected the carboxylic groups behave as weak acid groups (i.e., apparent pK_a values in the range of 5-7) and regardless of the amounts of counter-ions that are present within the aqueous phase, the uptake of sodium is markedly dependent on pH over a wide range of pH conditions. A balance between the degree of resin dissociation and counter-ion exchange with the aqueous phase remains over a broad range of pH conditions. The predictions using the simple numerical model are also shown and agree with the data reasonably well considering the various simplifying assumptions involved. Only one ring type is present and it contains one ionogenic group (i.e., a carboxylic group). A pK_a value of 5.0 was employed, along with a fixed value for the Na-H selectivity coefficient of 1.0.

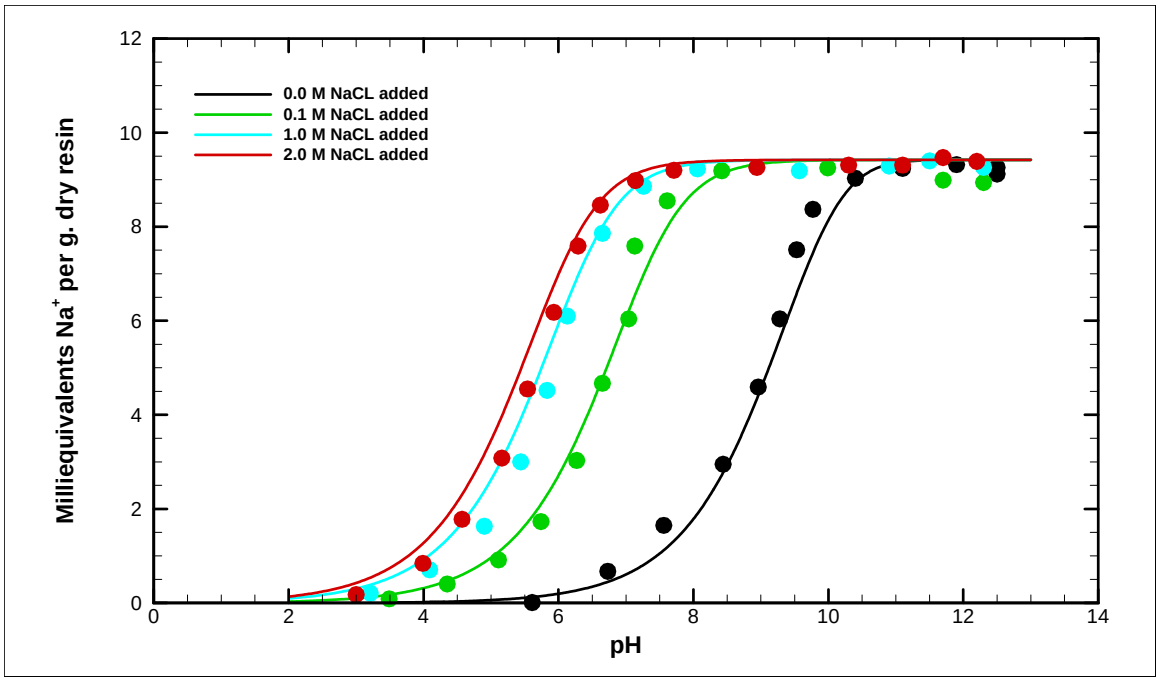

Figure 4.9 Comparison of simple numerical isotherm model to cross-linked polymethacrylic acid resin data taken by Hale and Reichenberg (1949).

4.6.2 Polyfunctional Resins

Given the success observed with predicting monofunctional resins (both strong and weak acid resins), our second assessment of the simple numerical model was the prediction of the behavior of the several polyfunctional resins tested by Topp and Pepper (1949). Our first assessment of the simple numerical model in predicting the behavior of a polyfunctional resin was based on a resin with two sites on its ring (i.e., the phenolic OH groups on the resorcinol-formaldehyde ring). Only one ring type was assumed to be present.

This polyfunctional resin is considered to be a very weak acid resin since its apparent pK_a values are in the range of 9-10 for the first phenolic site to dissociate and in the range of 10-12 for the second phenolic site to dissociate. The sodium uptake data are plotted in Figure 4.10 along with those for a very similar monofunctional resin (i.e., phenol-formaldehyde with a single phenolic OH site per ring). The predictions using the simple numerical model are also shown and agree with the data reasonably well considering the various simplifying assumptions involved.

For the phenol-formaldehyde resin only one ring type is present and it contains one ionogenic group (i.e., a phenolic group). A pK_a value of 11.5 was employed, along with a fixed value for the Na-H selectivity coefficient of 1.0. For the resorcinol-formaldehyde resin only one ring type is present and it contains one ionogenic group (i.e., a phenolic group). However, two sites exist per ring and their electrochemical properties shift depending upon level of dissociation present. Apparent pK_a values of 10.0 and 12.0 were employed, along with a fixed value for the Na-H selectivity coefficient of 1.0. Though not reported by Topp and Pepper (1949), the resorcinol-formaldehyde data may have had a small amount of carboxylic groups present given the shape of their data in the pH 6-11 range.

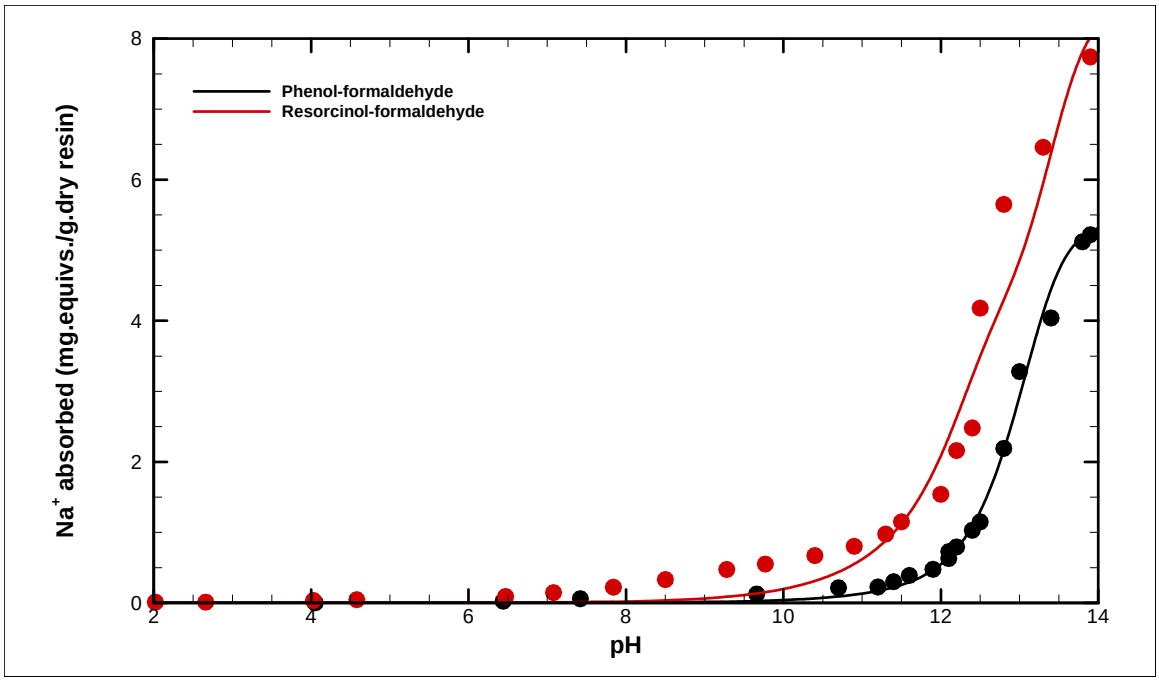

Figure 4.10 Comparison of simple numerical isotherm model to phenol-formaldehyde and resorcinol-formaldehyde resin data taken by Topp and Pepper (1949).

If we plot the sodium uptake loadings for these two resin types on a ring basis, we see some level of consistency in their pKa value for the first phenolic site.

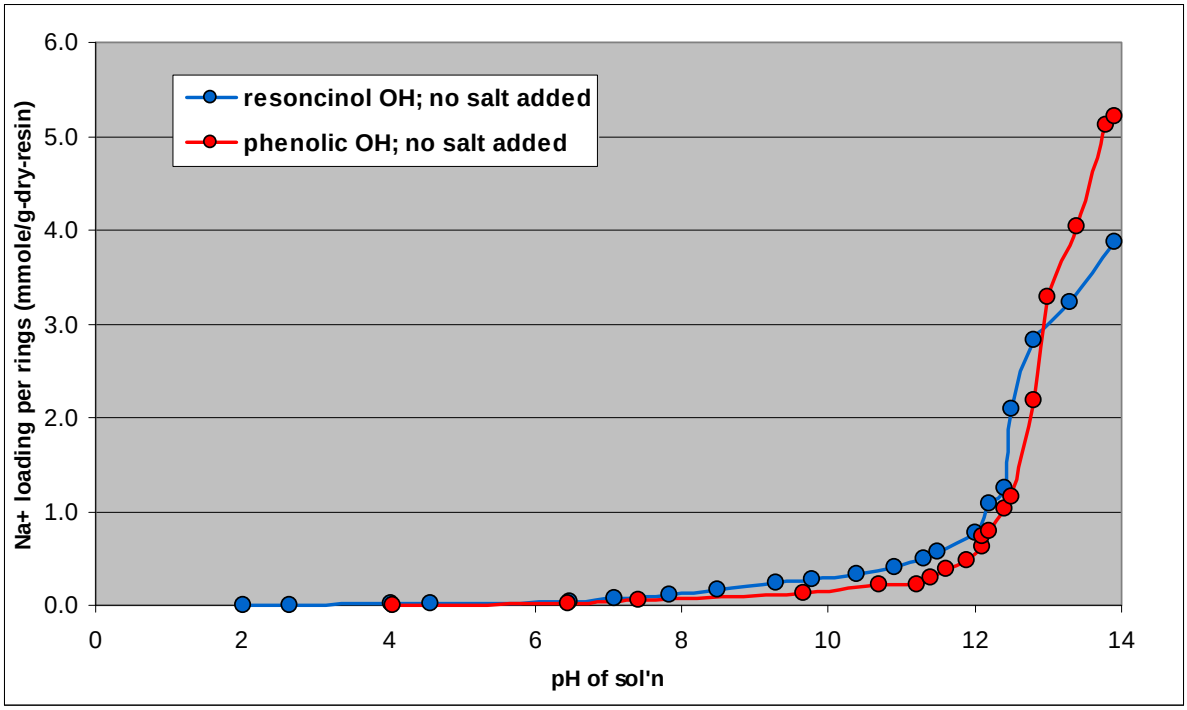

Figure 4.11 Comparison of phenol-formaldehyde and resorcinol-formaldehyde resin data based on sites per ring taken by Topp and Pepper (1949).

Our second assessment of the simple numerical model in predicting the behavior of a polyfunctional resin was based on a resin with two rings types (i.e., the phenolic OH groups on the phenol-formaldehyde ring and sulfonic SO_3H groups) each having only one site per ring. This polyfunctional resin is considered to be a mixture of strong and weak acid resins since its apparent pK_a values are in the range of -1 to 1 for the sulfonic site to dissociate and in the range of 9-10 for the phenolic site to dissociate. The sodium uptake data are plotted in Figure 4.12. Given the drastic difference in the two ionogenic group's pK_a values, their signatures on a titration curve are very easily spotted.

The predictions using the simple numerical model are also shown and agree with the data reasonably well considering the various simplifying assumptions involved. Assuming one sulfonic group on a ring, a pK_a value of -0.9 was employed, along with a fixed value for the Na-H selectivity coefficient of 1.0. Assuming one phenolic group on a ring a pK_a value of 10.0 was employed, along with a fixed value for the Na-H selectivity coefficient of 1.0. For this case we set the fraction of available rings per type equal. This should be fairly close to their actual values since the titration curve indicates each ring type capacity level fairly clearly.

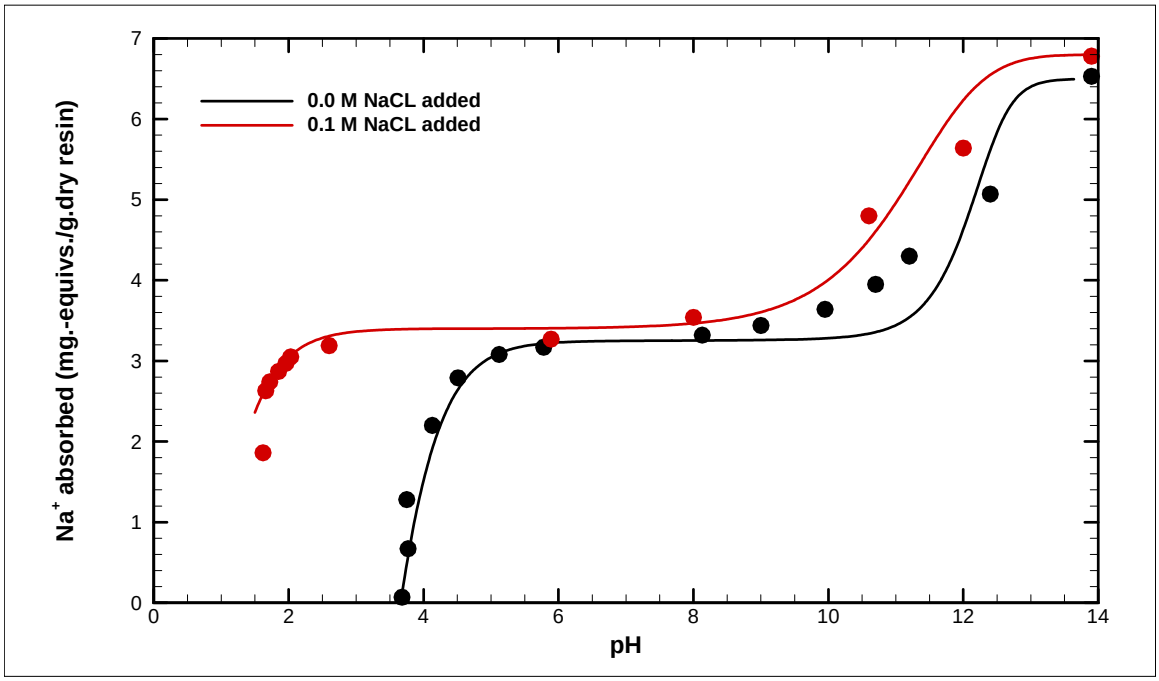

Figure 4.12 Comparison of simple numerical isotherm model to sulfated phenol-formaldehyde resin data taken by Topp and Pepper (1949).

Our third assessment of the simple numerical model in predicting the behavior of a polyfunctional resin was based on a resin tested by Topp and Pepper (1949) where both carboxylic COOH groups and resorcylic OH groups were present. The actual arrangement of these ionogenic groups among various possible ring types is unclear. The following two configurations are considered below:

- One ring type assumed where one carboxylic group and two phenolic groups are present on each ring; and

- Two ring types assumed where one ring type contains a single carboxylic group while the other ring type contains the two phenolic groups (resorcylic groups).

In both interpretations, this polyfunctional resin is considered to be a mixture of weak and very weak acid resins since its apparent pK_a values are in the range of 4 to 7 for the carboxylic site to dissociate and in the range of 9-12 for the resorcylic sites to dissociate. The potassium uptake data are plotted (as filled circles) in Figure 4.13. The hump seen around pH of 8 reflects the presence of the carboxylic groups

The predictions using the simple numerical model are also shown and agree with the data reasonably well considering the various simplifying assumptions involved. The results are based on the single ring interpretation where for the carboxylic group, a pK_a value of 4.9 was employed, along with a fixed value for the K-H selectivity coefficient of 1.0. For the two resorcylic groups pK_a values of 8.8 and 11.0 were employed, along with a fixed value for the K-H selectivity coefficient of 1.0.

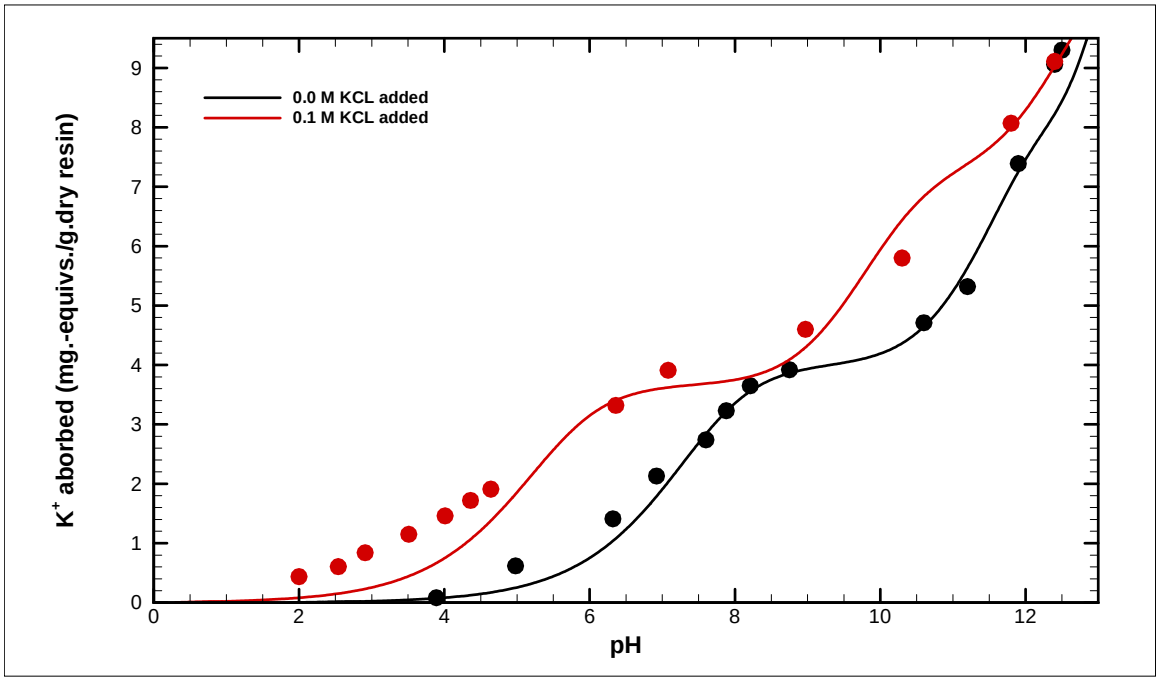

Figure 4.13 Comparison of simple numerical isotherm model to a resin containing carboxylic and resorcylic groups (on same ring type) (data taken by Topp and Pepper, 1949).

To illustrate the effect of interpreting the ring types differently, the predictions using the simple numerical model are shown in Figure 4.14 for this same resin where two ring types are assumed. The first ring type contains a single carboxylic group with a pK_a value of set to 4.5, along with a fixed value for the K-H selectivity coefficient of 1.0. The second ring type contains the two resorcylic groups with pK_a values set to 8.8 and 11.0, along with a fixed value for the K-H selectivity coefficient of 1.0. For this case, we assume equal fractions of available ring types.

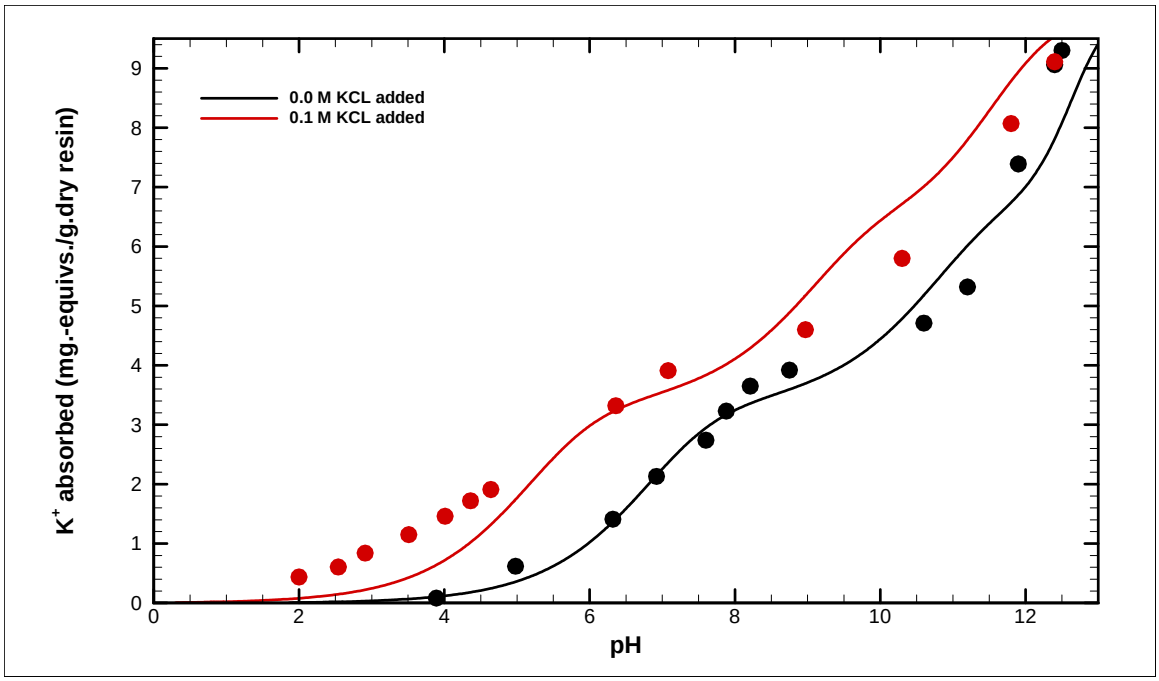

Figure 4.14 Comparison of simple numerical isotherm model to a resin containing carboxylic and resorcylic groups (on different ring types) (data taken by Topp and Pepper, 1949).

Our fourth and last assessment of the simple numerical model in predicting of the behavior of a polyfunctional resin was based on another resin tested by Topp and Pepper (1949) where nuclear sulfonic groups, carboxylic COOH groups, and resorcylic OH groups were present. The actual arrangement of these ionogenic groups among various possible ring types is unclear. The following two configurations are considered below:

- Two ring types assumed where one ring type contains a single sulfonic group while the other ring type contains a single carboxylic group in addition to two phenolic groups (resorcylic groups); and
- Three ring types assumed where the first ring type contains a single sulfonic group, the second ring type contains a single carboxylic group, and the third ring type contains the two phenolic groups (resorcylic groups).

We believe that the first interpretation listed above represents a close approximation to the ring types present within sRF. Note that Topp and Pepper (1949) do not provide sufficient information for estimating the actual ring type present or the number fractions of the ring types.

In both interpretations, this polyfunctional resin is considered to be a mixture of strong, weak, and very weak acid resins since its apparent pK_a values are in the range of -1 to 1 for the sulfonic site to dissociate, in the range of 4-7 for the carboxylic site to dissociate, and in the range of 9-12 for the resorcylic sites to dissociate. The potassium uptake data are plotted (as filled circles) in Figure 4.15. The expected hump at intermediate pH values due to carboxylic groups is not clearly seen within this data set. However, a slight indication may be seen near the data point of pH=7.2 (i.e., in the absence of a neutral salt).

The predictions using the simple numerical model are also shown and limited agreement with the data is observed. The results are based on the two ring type interpretation where for the sulfonic

group on the first ring type, a pK_a value of -1.0 was employed, along with a fixed value for the K-H selectivity coefficient of 2.5. For the carboxylic group on the second ring type a pK_a value of 5.5 was employed, while the two resorcylic group pK_a values were set to 9.0 and 11.3, along with a fixed value for the K-H selectivity coefficient of 1.0. For this case we set the fraction of available rings per type equal (i.e., 50% each).

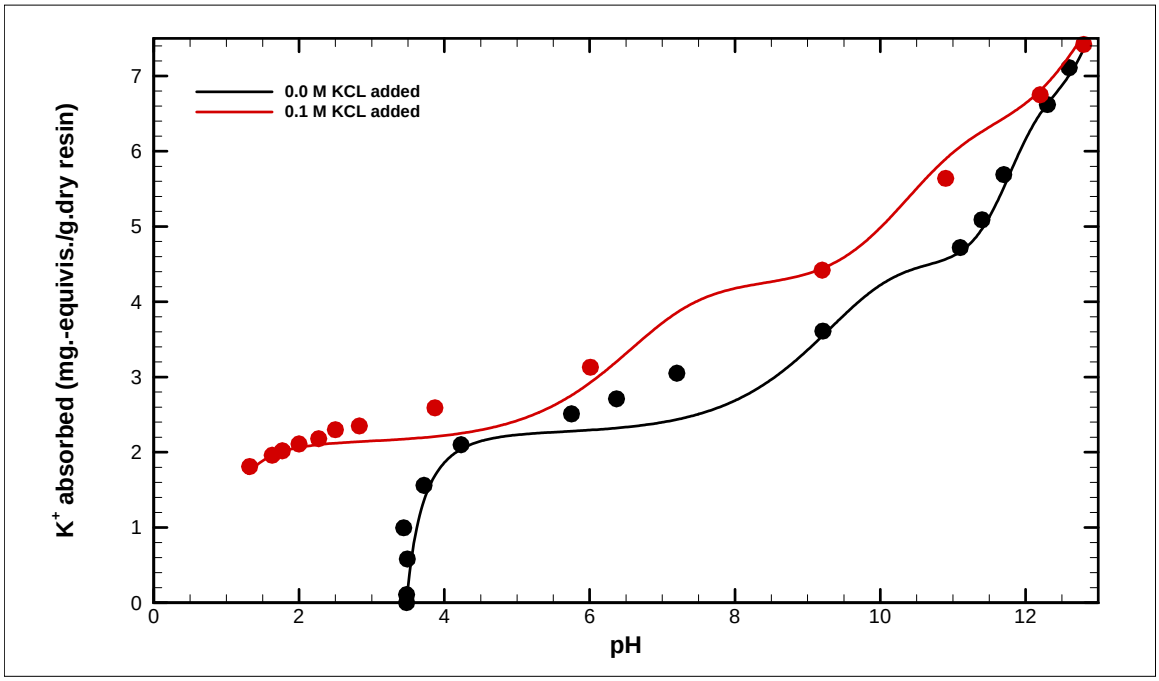

Figure 4.15 Comparison of simple numerical isotherm model to a resin containing sulfonic, carboxylic, and resorcylic groups (2 ring types assumed) (data taken by Topp and Pepper, 1949).

As done above, to illustrate the effect of interpreting the ring types differently, the predictions using the simple numerical model are shown in Figure 4.16 for this same resin where three ring types are assumed. The first ring type contains a single sulfonic group with a pK_a value set to 0.9, along with a fixed value for the K-H selectivity coefficient of 1.0. The second ring type contains a single carboxylic group with pK_a values set to 4.5, along with a fixed value for the K-H selectivity coefficient of 1.0. The third ring type contains the two resorcylic groups with pK_a values set to 10.0 and 12.0, along with a fixed value for the K-H selectivity coefficient of 1.0. For this case we set the fraction of available rings per type equal (i.e., 33.3% each)

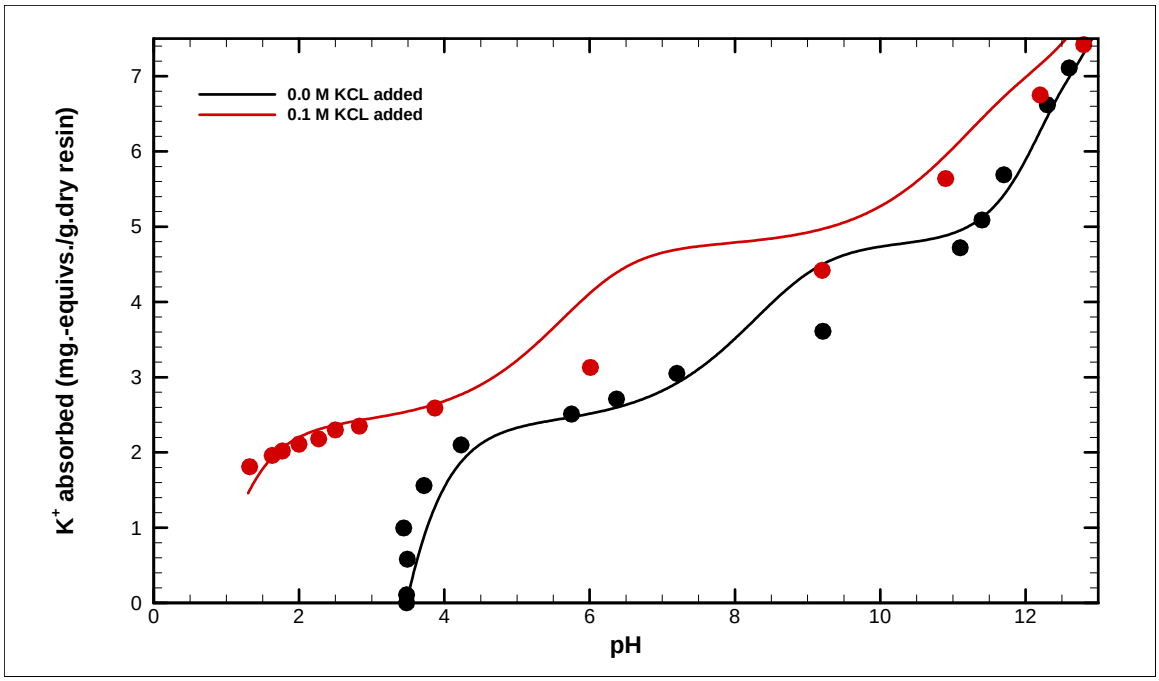

Figure 4.16 Comparison of simple numerical isotherm model to a resin containing sulfonic, carboxylic, and resorcylic groups (3 ring types assumed) (data taken by Topp and Pepper, 1949).

5.0 Conclusions and Recommendations

Work conducted in FY2011 has resulted in a fundamental change in the approach to ion-exchange modeling. Previous work used widely accepted isotherm models such as the Langmuir or Freundlich/Langmuir forms to represent the ion-exchange mechanism. These isotherms are more appropriate for adsorption processes and the Langmuir isotherm can be easily derived by assuming equilibrium between the rates of adsorption and desorption from a surface. While this approach was successful in modeling experimental results for ion-exchange column loading it cannot be readily extended to include column elution except by developing another isotherm applicable under elution conditions. For the applications of interest to the Hanford SCIX and WTP processes and at SRS, column loading takes place in a high pH caustic environment while column elution requires a low pH acidic environment. In principle, it should be possible to capture the behavior of the ion-exchange resin over the entire range of pH within a single model. In general terms, at high pH the resin should show an affinity for cesium while at low pH the cesium and other ions are displaced by hydrogen ions. As demonstrated in Section 4, the model should also be capcable of modeling ion-exchange in the presence of high concentraitons of other ions such as Na^+ and K^+.

Preliminary work performed in 2011 has moved ion-exchange modeling in the direction outlined above. A mass-action isotherm model that uses equations appropriate for ion-exchange is under development. This work builds on previous work at SRNL by Aleman and Hamm which developed a thermodynamic based model of ion-exchange that was used in conjunction with experimental data to derive parameters for Langmuir or Freundlich/Langmuir isotherms. The model accounts for ion activities in solution and activities when complexed with the solid resin. As discussed in Section 4, this model is being revised to calculate parameters for a mass-action based isotherm. Preliminary work in this area is very encouraging that this model will capture ion-exchange behavior over a wide range of solution pH. Trial calculations of column performance using a mass-action isotherm have been made as shown in Section 3.3 of this report. Again, these preliminary calculations are very encouraging that the entire ion-exchange cycle from column loading to column elution can be successfully modeled.

Use of the mass-action modeling approach provides significant benefits. The groundwork laid down by the work can be improved by additional development of the mass-action isotherm model and simulations of the full column cycle. Recommendations for future modeling work are:

1. Complete development of theoretical mass-action isotherm model based on the CERMOD code previously developed at SRNL.
2. Use experimental data to predict mass-action isotherms for column loading, rinsing, and elution.
3. Run column simulations of the entire ion-exchange cycle for elutable sRF using the mass-action isotherm and compare model predictions to experimental data.

6.0 References

Aleman, S.E. and L.L. Hamm, 2007, "CERMOD Version 1.1: Detailed Thermodynamic Equilibrium Model for the Prediction of Ion Exchange Behavior on Monovalent Cation Exchange Resins," WRSC-STI-2007-00054, Savannah River National Laboratory, Aiken, SC 29808.

Aleman, S.E., L.L. Hamm and F.G. Smith, 2007, "Ion Exchange Modeling of Cesium Removal from Hanford Waste Using Spherical Resorcinol Formaldehyde Resin," WSRC-STI-2007-00030, Savannah River National Laboratory, Aiken, SC 29808.

Bauman, W.C., 1946, "Improved Synthetic Ion Exchange Resin," Ind. and Engr. Chem., Vol. 38, No. 1, p. 47.

Bauman, W.C. and J. Eichhorn, 1947, "Fundamental Properties of a Synthetic Cation Exchange Resin," Ind. J. Am. Chem. Soc., Vol. 69, p. 2830.

Bauman, W.C., J.R. Skidmore and R.H. Osmun, 1948, "DOWEX 50: A New High Capacity Cation Exchange Resin," Ind. and Engr. Chem., Vol. 40, No. 8, p. 1350.

Berninger, J., R.D. Whitley, X. Zhang and N.-H.L. Wang, 1991, "A Versatile Model for Simulation of Reaction and Nonequilibrium Dynamics in Multicomponent Fixed Bed Adsorption Processes," Comput. Chem. Eng., 15(11), 749-768.

Bibler, J.P., R.M. Wallace and L.A. Bray, 1990, Proceedings of Symposium on Waste Management (Waste Management '90). HLW and LLW Technology, II, p. 747.

Birdwell, J., D. Schuh, P. Taylor, R. Collins and R. Hunt, 2010, "An Engineering Evaluation of Spherical Resorcinol Formaldehyde Resin", ORNL/TM-2010/200, Oak Ridge National Laboratory, Oak Ridge, TN 37831.

Brown, G.N., R.L. Russel and R.A. Peterson, 2011, "Small-Column Ion Exchange Testing of Spherical Resorcinol-Formaldehyde," Proceedings of Symposium on Waste Management (Waste Management '11). HLW and LLW Technology, 11379.

Cornaz, J.P., and H. Deuel, 1956, Helv. Chim. Acta, Vol. 39, p. 1227.

Ernest, M.V., R.D. Whitley, Z. Ma and N.H.L. Wang, 1997, "Effects of Mass Action Equilibrium on Fixed-Bed Multicomponent Ion-Exchange Dynamics," Ind. Eng. Chem. Res., Vol. 36, p. 212.

Fiskum, S.K., S.T. Arm, M.S. Fountain, M.J. Steele and D.L. Blanchard, Jr, 2006, "Spherical Resorcinol-Formaldehyde Resin Testing for 137Cs Removal from Simulated and Actual Hanford Waste Tank 241-AP-101 Diluted Feed (Envelope A) Using Small Column Ion Exchange,", WTP-RPT-134, Battelle, Pacific Northwest Division, Richland, WA 99352.

Fondeur, F.F., W.D. King, S. W. McCollum and M.A. Pettis, 2006, "Spherical Resorcinol-Formaldehyde Resin Reactivity with Nitric Acid and Other Hanford RPP-WTP Process Solutions" WSRC-TR-2005-00228, Savannah River National Laboratory, Aiken, SC 29808.

Gregor, H.P. and J.I. Bregman, 1948, "Characterization of Ion Exchange Resins. I. Acidity and Number of Constituent Cation Exchange Groups," J. Am. Chem. Soc., Vol. 70, p. 2370.

Hale, D.K. and D. Reichenberg, 1949, "Equilibrium and Rate Studies of Cation-Exchange with Monofunctional Resins," Discussions Faraday Soc., Vol. 7, p. 79.

Helfferich, F.G., 1962, Ion Exchange, McGraw-Hill Series in Advanced Chemistry, republished in 1965 and in 1995 by Dover Publications, Inc.

Hubler, T.L., J.A. Franz, W.J. Shaw, S.A. Bryan, R.T. Hallen, G.N. Brown, L.A. Bray and J.C. Linehan, 1995, "Synthesis, Structural Characterization, and Performance Evaluation of Resorcinol-Formaldehyde (R-F) Ion-Exchange Resin," Pacific Northwest Laboratory, PNL-10744 (UC-721).

Hubler, T.L., J.A. Franz, W.J. Shaw, M.O. Hogan, R.T. Hallen, G.N. Brown and J.C. Linehan, 1996, "Structure/Function Studies of Resorcinol-Formaldehyde (R-F) and Phenol-Formaldehyde (P-F) Copolymer Ion-Exchange Resins," Pacific Northwest Laboratory, PNNL-11347 (UC-721).

Nash, C. A and Isom, 2010, Personal communication and spreadsheet.

Nash, C. A and A. Polite, 2011, Personal communication and spreadsheet.

Smith, F.G., 2007, "Modeling of Ion-Exchange for Cesium Removal from Dissolved Saltcake in SRS Tanks 1-3, 37 and 41," WSRC-STI-2007-00315, Savannah River National Laboratory, Aiken, SC 29808.

Taylor, P.A. and H.L. Johnson, 2009, "Alternate Methods for Eluting Cesium from Spherical Resorcinol-Formaldehyde Resin," ORNL/TM-2008/194, Oak Ridge National Laboratory, Oak Ridge, TN 37831.

Topp, N.E. and K.W. Pepper, 1949, "Properties of Ion-exchange Resins in Relation to their Structure. Part I. Titration Curves," J. Chem. Soc., p. 3299.

Whitley, R.D. and N.-H.L. Wang, 1998, "User's Manual VERSE (VErsatile Reaction SEparation) Simulation for Liquid Phase Adsorption and Chromatography Processes," School of Chemical Engineering, Purdue University.

Appendix A: Tabulation of Column Experiments

	Report	Year	Run No.	Elution M HNO3	Elution BV/hr	Resin Batch	Solution	Experimental Conditions	Experimental Data	Comment
1	**WTP-RPT-134**	2006		0.50	1.50	5E-370/641	AP-101 Sim	Table 2.3	Table D.1 & D.2	
2				0.50	1.42	5E-370/641	AP-101 ADF	Table 2.3	Table D.3 & D.4	
3	**WTP-RPT-135**	2006		0.50	1.41	5E-370/641	AN-102 AW	Table 2.5	Table B.1	10% breakthrough, used column
4	**WTP-RPT-143**	2006	Wave 3	0.25	1.41	5E-370/639	AP-101 Sim	Table 11.6	Table 11.10	different resin batch
5				0.40	1.41	5E-370/641	AP-101 Sim	Table 11.7	Table 11.11	duplicates 134
6			Wave 3a	0.50	1.40	5E-370/641	AP-101 Sim	Table 12.2	Table 12.6	upflow elution
7	**PNWD-3985**	2008	Wave 1	0.50	1.56	5E-370/641	DST-1	Table B.3		upflow elution, no data reported
8				0.50	1.87	5E-370/641	DST-1	Table B.1		upflow elution, no data reported
9				0.50	1.47	5E-370/641	DST-2	Table B.2		upflow elution, no data reported
10			Wave 2	0.50	1.90	5E-370/641	DST-1	Table B.7		upflow elution, no data reported
11				0.50	1.61	5E-370/641	DST-3	Table B.6		upflow elution, no data reported
12				0.50	1.62	5E-370/641	DS	Table B.5		upflow elution, no data reported
13				0.50	2.06	5E-370/641	DST-2	Table B.4		upflow elution, no data reported
14	**ORNL-194**	2009	2, 5, 12, 15	0.50	1.00	5E-370/641	SCIX Feed		Appendix B	no loading breakthrough
15			3, 13, 16	0.50/0.05	1.00	5E-370/641	SCIX Feed		Appendix B	no loading breakthrough
16			9	0.20	1.00	5E-370/641	SCIX Feed		Appendix B	no loading breakthrough
17			10	0.10	1.00	5E-370/641	SCIX Feed		Appendix B	no loading breakthrough
18			11	0.50	0.70	5E-370/641	SCIX Feed		Appendix B	no loading breakthrough
19			1	0.50	2.00	5E-370/641	SCIX Feed		Appendix B	no loading breakthrough
20	**SRNL-00024**	2006		0.50	1.27	5E-370/641	AP-101 Sim	Table 16		no data reported
21				0.50	1.34	5E-370/641	AN-107 Sim	Table 16		no data reported
22	**SRNL-00367**	2009		0.50	1.40	5E-370/641	Tank 2F Sim			no data reported
23				0.50	1.40	5E-370/641	Real Waste			no data reported
24	**PNNL WM**	2011		0.02	1.40	5E-370/641	Simple Sim			2% breakthrough, no data reported
25				0.07	1.40	5E-370/641	Simple Sim			2% breakthrough, no data reported
26				0.15	1.40	5E-370/641	Simple Sim			2% breakthrough, no data reported
27				0.23	1.40	5E-370/641	Simple Sim			2% breakthrough, no data reported
28				0.28	1.40	5E-370/641	Simple Sim			2% breakthrough, no data reported

Appendix B: Simple Deprotonation Model

As stated within the main body of the report, a simplified deprotonation model was employed to assist in developing a better understanding of the sRF resin over the entire pH range of expected column operations. The details of this model are provided within this appendix. This simple model is the foundation upon which more detailed and complete models are envisioned. Its success is illustrated within the main body of the report.

Currently loading, displacement, washing, elution, and regeneration process steps are envisioned where the span in pH is from the loading step of 12-14 pH down to the elution step of 0-1 pH. The other three steps are at intermediate pH ranges. Elution is planned to be performed using ~0.5 M HNO_3 while loading of 5+ M Na^+ solutions in the presence of ~0-2 M OH^-. It should also be pointed out that various studies have been undertaken or proposed where the operating range is altered. For example, 8+ M Na^+ solutions had been considered or recycled HNO_3 with possibly a lower acid strength used.

Early on elution data indicated that the apparent capacity of sRF for Na^+ is in the range of 6-7 mmole-equivalents per gram of dry H-form resin (i.e, for batch 5E-370/641). Batch contact data at high pH values (i.e., pH>11) indicated that the following cationic loadings were achievable for:

- Na^+ of 6-7 mmole-equivalents per gram of dry H-form resin; and
- Cs^+ of 0.6 to 0.7 mmole-equivalents per gram of dry H-form resin in 6 M Na solution.

As seen above the Na^+ ionic capacities were consistent between the two test methods and the scientific weight capacity of sRF for Na^+ is believed to correspond to this range of values. However, the Cs^+ apparent capacity can be seen to be approximately one order in magnitude lower than our believed scientific weight capacity of the ionogenic groups. Steric-like effects were believed to be the reason for this apparent capacity reduction.

In the simple deprotonation model it is assumed that each benzene ring containing one or more ionogenic groups (i.e., ionizable groups in the sense of acid-like disassociation), is electrochemically independent of all the other benzene rings bound in the three-dimensional hydrocarbon network (i.e., resin solid phase). Here effective electronic and electrostatic shielding between monomer units is achieved. However, within a given ring containing multiple ionogenic groups their pK_a values can vary indicative of electrochemical interactions. As discussed within the main body of this report, these assumptions allow the separation of resin into different resin types whose rings are all of a specific type. The overall resin is then obtained by simple mixing (i.e., summing up each one's contribution).

Again, since only a simple conceptual based model is being considered here, resin phase and aqueous phase activity coefficients are not being addressed. Thus activities of every species are being set equal to their appropriately defined phasic concentrations.

Given our current understanding of sRF, three ring types are considered here:

- Rings containing 1-site;
- Rings containing 2-sites; and
- Rings containing 3-sites;

Below the equations describing each of these ring types are provided.

B.1 One-Site Ring Deprotonation Model

The ionization reaction for the resin (i.e., the disassociation of the one ionogenic group and sometimes referred to as a resinate) can be expressed as:

$$RH \overset{K_1}{\leftrightarrow} R^- + \overline{H}^+ \tag{B-1}$$

which in equation form becomes:

$$K_1 = \frac{[R^-][\overline{H}^+]}{[RH]} \tag{B-2}$$

where

- K_1 - Ionization constant for the specified reaction.
- $[RH]$ - Ring concentration with unionized ionogenic group in terms of mmol/ml.
- $[R^-]$ - Ring concentration with ionized ionogenic group in terms of mmol/ml.
- $[\overline{H}^+]$ - Concentration of H^+ ion within the resin phase as defined by its Donnan potential field surrounding the resin in terms of mmol/ml.

For disassociation reaction, such as Eq. (B-1), the ionization constant is typically provided within the literature in terms of a pKa value defined as:

$$pKa_i = -\log_{10} K_i$$

and the pH is being approximated here by:

$$pH = -\log_{10} a_H \approx -\log_{10}[H] \quad \text{(for the aqueous solution)}$$

$$p\overline{H} = -\log_{10} a_{\overline{H}} \approx -\log_{10}[\overline{H}] \quad \text{(for the resin phase)}$$

The valance charges have been omitted for clarity. Note that the standard state chosen for the resonates (i.e., ring states) is on a per gram of dry resin in its pure H-form. The specific volume for the resin in its saturated (wet) state where the uptake of water solvent has reached its equilibrium value is:

- $\underline{V}$ - Specific volume of resin phase in terms of milliliter per gram of dry resin in its pure H-form (ml/g_{resin}).

The disassociation reaction for water in the aqueous solution takes the form:

$$H_2O \overset{K_w}{\leftrightarrow} OH^- + H^+ \tag{B-3}$$

which, in equation form, becomes:

$$K_w = [OH^-][H^+] \quad \text{(B-4)}$$

where

- K_w - Disassociation constant for the water (assumed here as 10^{-14}).
- $[H^+]$ - Concentration of H^+ ion within the aqueous phase in terms of mmol/ml.
- $[OH^-]$ - Concentration of OH^- ion within the aqueous phase in terms of mmol/ml.

The activity (concentration) of water has been incorporated into the water disassociation constant in Eq. (B-4). The total concentration of rings (both unionized and ionized ring states) becomes:

$$[R_T] = [RH] + [R] \quad \text{(B-5)}$$

where

- R_T - Concentration of total rings present within resin phase that contains ionogenic groups (mmol/ml).

Note that this concentration only refers to those rings present within the resin phase that have ionogenic groups that are capable of having ion-exchange if ionized (i.e., steric effects could eliminate a ring or a ring may have no ionogenic groups).

Equation (B-5) can be recast using Eq. (B-2) into expressions stating the fraction of rings in the various possible ring states:

$$\alpha_0 \equiv \frac{[RH]}{[R_T]} = \frac{[\overline{H}]}{K_1 + [\overline{H}]} \quad \text{(no ionized site)} \quad \text{(B-6a)}$$

$$\alpha_1 \equiv \frac{[R]}{[R_T]} = \frac{K_1}{K_1 + [\overline{H}]} \quad \text{(one ionized site)} \quad \text{(B-6b)}$$

where conservation of the total number of ring states available implies:

$$\alpha_0 + \alpha_1 = 1 \quad \text{(B-7)}$$

The total concentration of rings present can be related to the scientific weight capacity of the resin's ionogenic groups by:

$$[Q_T] = [R_T]\underline{V} \quad \text{(B-8)}$$

where

- Q_T - Scientific weight capacity of ionogenic groups (mmol/ g_{resin});

and it has been assumed that only 1-site exists per available ring.

The resin consists of a cross-linked, high-polymer structure to which rings with ionizable groups are attached. These groups can be viewed as insoluble acids. As such the concentration of H^+ ions within their vicinity (i.e., within the resin structure) will generally be quite different than the

concentration of H^+ ions within the neighboring aqueous phase. However, for the conceptual purposes of this simple model we will make the following assumption:

$$[\overline{H}] \approx [H] \tag{B-9}$$

Making use of Eqs. (B-4) and (B-9), Eqs. (B-6) can be recast into the form:

$$\alpha_0 \equiv \frac{[RH]}{[R_T]} = \frac{1}{1+\beta_1[OH]} \tag{B-10b}$$

$$\alpha_1 \equiv \frac{[R]}{[R_T]} = \frac{\beta_1[OH]}{1+\beta_1[OH]} \tag{B-10a}$$

where

$$\beta_i \equiv \frac{K_i}{K_w}$$

The fraction of ionized sites (i.e., active sites) follows from Eqs. (B-10) as:

$$f_a = \frac{0\cdot[RH]+1\cdot[R]}{[R_T]} = 0\cdot\alpha_0 + 1\cdot\alpha_1 \tag{B-11}$$

where we see that only one ring state is active and that ring state contains only one site per ring.

B.2 Two-Site Ring Deprotonation Model

The 2-site model assumes that two different ionizable sites exist on the specific ring type considered. These ionizable sites can be of the same ionogenic group or different ionogenic types. In either case their pK_a values are assumed to be constant values but possibly different. For convention the first site is set to the ionogenic group with the lower pK_a value:

$$pKa_1 < pKa_2$$

The ionization reactions for the resin can be expressed as:

$$RH_2 \overset{K_1}{\leftrightarrow} RH^- + \overline{H}^+ \tag{B-11a}$$

$$RH^- \overset{K_2}{\leftrightarrow} R^{-2} + \overline{H}^+ \tag{B-11b}$$

which in equation form becomes:

$$K_1 = \frac{[RH^-][\overline{H}^+]}{[RH_2]} \tag{B-12a}$$

$$K_2 = \frac{[R^{-2}][\overline{H}^{+}]}{[RH^{-}]} \tag{B-12a}$$

where

- K_1 - Ionization constant for the first ionogenic group.
- K_2 - Ionization constant for the second ionogenic group.
- $[RH_2]$ - Ring concentration with unionized ionogenic groups in terms of mmol/ml.
- [RH] - Ring concentration with first ionogenic group ionized in terms of mmol/ml.
- [R] - Ring concentration with both ionogenic groups ionized in terms of mmol/ml.

The total concentration of rings (both unionized and ionized) becomes (i.e., three types of ring states):

$$[R_T] = [RH_2] + [RH] + [R] \tag{B-13}$$

Equation (B-13) can be recast using Eqs. (B-12) into expressions stating the fraction of rings in the two possible ionized ring states and the one unionized ring state:

$$\alpha_0 \equiv \frac{[RH_2]}{[R_T]} = \frac{[\overline{H}]^2}{K_1K_2 + K_1[\overline{H}] + [\overline{H}]^2} \tag{B-14a}$$

$$\alpha_1 \equiv \frac{[RH]}{[R_T]} = \frac{K_1[\overline{H}]}{K_1K_2 + K_1[\overline{H}] + [\overline{H}]^2} \tag{B-14b}$$

$$\alpha_2 \equiv \frac{[R]}{[R_T]} = \frac{K_1K_2}{K_1K_2 + K_1[\overline{H}] + [\overline{H}]^2} \tag{B-14c}$$

where for conservation of the total number of ring states available implies:

$$\alpha_0 + \alpha_1 + \alpha_2 = 1 \tag{B-15}$$

The total concentration of rings present can be related to the scientific weight capacity of the resin's ionogenic groups by:

$$[Q_T] = 2[R_T]\underline{V} \tag{B-16}$$

where

- Q_T - Scientific weight capacity of ionogenic groups (mmol/ g_{resin}).

and it has been assumed that only 2-sites exist per available ring.

Consistent with the 1-site case above, for the conceptual purposes of this simple model we will make the following assumption:

$$[\overline{H}] \approx [H] \tag{B-17}$$

Making use of Eqs. (B-4) and (B-17), Eqs. (B-14) can be recast into the form:

$$\alpha_0 \equiv \frac{[RH_2]}{[R_T]} = \frac{1}{1+\beta_1[OH]+\beta_1\beta_2[OH]^2} \quad \text{(B-18a)}$$

$$\alpha_1 \equiv \frac{[RH]}{[R_T]} = \frac{\beta_1[OH]}{1+\beta_1[OH]+\beta_1\beta_2[OH]^2} \quad \text{(B-18b)}$$

$$\alpha_2 \equiv \frac{[R]}{[R_T]} = \frac{\beta_1\beta_2[OH]^2}{1+\beta_1[OH]+\beta_1\beta_2[OH]^2} \quad \text{(B-18c)}$$

The fraction of ionized sites (i.e., active sites) follows from Eqs. (B-18) as:

$$f_a = \frac{0\cdot[RH_2]+1\cdot[RH]+2\cdot[R]}{[R_T]} = 0\cdot\alpha_0+1\cdot\alpha_1+2\cdot\alpha_2 \quad \text{(B-19)}$$

B.3 Three-Site Ring Deprotonation Model

The 3-site model assumes that three different ionizable sites exist on the specific ring type considered. All other assumptions are consistent with the above 1-site and 2-site models. For convention the first site is set to the ionogenic group with the lower pK_a value:

$$pKa_1 < pKa_2 < pKa_3$$

The ionization reactions for the resin can be expressed as:

$$RH_3 \overset{K_1}{\leftrightarrow} RH_2^- + \overline{H}^+ \quad \text{(B-20a)}$$

$$RH_2^- \overset{K_2}{\leftrightarrow} RH^{-2} + \overline{H}^+ \quad \text{(B-20b)}$$

$$RH^{-2} \overset{K_3}{\leftrightarrow} R^{-3} + \overline{H}^+ \quad \text{(B-20c)}$$

where in equation form becomes:

$$K_1 = \frac{[RH_2^-][\overline{H}^+]}{[RH_3]} \quad \text{(B-21a)}$$

$$K_2 = \frac{[RH^{-2}][\overline{H}^+]}{[RH_2^-]} \quad \text{(B-21b)}$$

$$K_3 = \frac{[R^{-3}][\overline{H}^+]}{[RH^{-2}]} \quad \text{(B-21c)}$$

where

- K_1 - Ionization constant for the first ionogenic group.
- K_2 - Ionization constant for the second ionogenic group.
- K_3 - Ionization constant for the third ionogenic group.
- $[RH_3]$ - Ring concentration with unionized ionogenic groups in terms of mmol/ml.
- $[RH_2]$ - Ring concentration with first ionogenic group ionized in terms of mmol/ml.
- [RH] - Ring concentration with first and second ionogenic group ionized in terms of mmol/ml.
- [R] - Ring concentration with all ionogenic groups ionized in terms of mmol/ml.

The total concentration of rings (both unionized and ionized) becomes (i.e., four types of ring states):

$$[R_T] = [RH_3] + [RH_2] + [RH] + [R] \tag{B-22}$$

Equation (B-22) can be recast using Eqs. (B-21) into expressions stating the fraction of rings in the three possible ionized ring states and the one unionized ring state:

$$\alpha_0 \equiv \frac{[RH_3]}{[R_T]} = \frac{[\overline{H}]^3}{K_1K_2K_3 + K_1K_2[\overline{H}] + K_1[\overline{H}]^2 + [\overline{H}]^3} \tag{B-23a}$$

$$\alpha_1 \equiv \frac{[RH_2]}{[R_T]} = \frac{K_1[\overline{H}]^2}{K_1K_2K_3 + K_1K_2[\overline{H}] + K_1[\overline{H}]^2 + [\overline{H}]^3} \tag{B-23b}$$

$$\alpha_2 \equiv \frac{[RH]}{[R_T]} = \frac{K_1K_2[\overline{H}]}{K_1K_2K_3 + K_1K_2[\overline{H}] + K_1[\overline{H}]^2 + [\overline{H}]^3} \tag{B-23c}$$

$$\alpha_3 \equiv \frac{[R]}{[R_T]} = \frac{K_1K_2K_3}{K_1K_2K_3 + K_1K_2[\overline{H}] + K_1[\overline{H}]^2 + [\overline{H}]^3} \tag{B-23d}$$

where for conservation of the total number of ring states available implies:

$$\alpha_0 + \alpha_1 + \alpha_2 + \alpha_3 = 1 \tag{B-24}$$

The total concentration of rings present can be related to the scientific weight capacity of the resin's ionogenic groups by:

$$[Q_T] = 3[R_T]\underline{V} \tag{B-25}$$

where

- Q_T - Scientific weight capacity of ionogenic groups (mmol/ g_{resin}).
- and here it has been assumed that only 3-sites per available ring exist.

Consistent with the 1-site and 2-site cases above, for the conceptual purposes of this simple model we will make the following assumption:

$$[\overline{H}] \approx [H] \tag{B-26}$$

Making use of Eqs. (B-4) and (B-26), Eq. (B-23) can be recast into the form:

$$\alpha_0 \equiv \frac{[RH_3]}{[R_T]} = \frac{1}{1+\beta_1[OH]+\beta_1\beta_2[OH]^2+\beta_1\beta_2\beta_3[OH]^3} \tag{B-27a}$$

$$\alpha_1 \equiv \frac{[RH_2]}{[R_T]} = \frac{\beta_1[OH]}{1+\beta_1[OH]+\beta_1\beta_2[OH]^2+\beta_1\beta_2\beta_3[OH]^3} \tag{B-27b}$$

$$\alpha_2 \equiv \frac{[RH]}{[R_T]} = \frac{\beta_1\beta_2[OH]^2}{1+\beta_1[OH]+\beta_1\beta_2[OH]^2+\beta_1\beta_2\beta_3[OH]^3} \tag{B-27c}$$

$$\alpha_3 \equiv \frac{[R]}{[R_T]} = \frac{\beta_1\beta_2\beta_3[OH]^3}{1+\beta_1[OH]+\beta_1\beta_2[OH]^2+\beta_1\beta_2\beta_3[OH]^3} \tag{B-27d}$$

The fraction of ionized sites (i.e., active sites) follows from Eqs. (B-18) as:

$$f_a = \frac{0\cdot[RH_3]+1\cdot[RH_2]+2\cdot[RH]+3\cdot[R]}{[R_T]} = 0\cdot\alpha_0+1\cdot\alpha_1+2\cdot\alpha_2+3\cdot\alpha_3 \tag{B-19}$$

B.4 Mixture Ring Deprotonation Model

As discussed in the main body of the report, the assumption that the electrochemical state of a ring is independent of all other ring states allows us to take all of the available rings within a given mass of resin and partition them out into different categories. For sRF, as mentioned earlier, the following categories are believed to be the dominant present:

- Rings with 1-site available (total of 2 ring states);
- Rings with 2-sites available (total of 3 ring states); and
- Rings with 3-sites available (total of 4 ring states);

Based on the above assumption of independence, the isotherm behavior of each category can be determined independently from the other categories. The overall composite isotherm relating the behavior of the entire resin material then becomes a simple summing up of the contributions from each category. Here knowledge of the number fraction of each ring type category is required to perform this summation.

The total ionic capacity of the entire resin can be defined based on the total number of available ionogenic groups present (on a per gram of dry resin basis and typically assumed standard state of the pure H-form). This capacity is referred to as the scientific weight capacity, Q_T (mmol/ g_{resin}). When there is only one ring type present as the above sections apply, the total number of available rings is related to this total ionic capacity based on the integer number of sites per ring (i.e., here, 1, 2, or 3 sites per ring). However, when there is a mixture of ring types present a more complicated (and most likely non-integer number) relationship exists between these two quantities.

The number of sites per ring type has been specified by convention to be:

$$n_1 = 1$$
$$n_2 = 2$$
$$n_3 = 3$$

where

- n_i - Number sites per ring of type i, (-).

In this report we shall define the mixture resin by specifying the number fractions of ring types present:

$$x_i \quad (i = 1,2,3)$$

where

- x_i - Number fraction of available ring types within resin (i.e., total number of rings of type i per total number of all available rings present).

By definition we have:

$$\sum_{i=1}^{3} x_i = 1 \tag{B-28}$$

These fractions specify the resin mixture allowing us the ability to address each ring type separately and then combining ring type results to estimate mixture behavior. The number of rings of a given ring type becomes:

$$[R_i] = x_i[R_T] \quad (i = 1,2,3) \tag{B-29}$$

where

- $[R_i]$ - Number rings of type i per ml of resin, (mmol/ml).
- $[R_T]$ - Total number of available rings within the resin per ml, (mmol/ml).

This total number of available rings within the resin becomes follows as:

$$[R_T] = \sum_{i=1}^{3} [R_i] \tag{B-30}$$

For each ring type the total number of disassociated sites (i.e., active sites) becomes:

$$Q_{ai} = f_{ai}[R_i] \tag{B-31}$$

where

- Q_{ai} - Total number of active sites for rings of type i per ml of resin, (mmol/ml).

The total number of active sites within the resin mixture then becomes:

$$Q_a = \sum_{i=1}^{3} Q_{ai} = \sum_{i=1}^{3} f_{ai}[R_i] \quad \text{(B-32)}$$

where

- Q_a - Total number of active sites per ml of resin, (mmol/ml).

From the above definitions we can relate the total number of available rings to the total number of available sites by the expression:

$$Q_T = \langle n \rangle [R_T] \underline{V} \quad \text{(B-31)}$$

where

$$\langle n \rangle = \sum_{i=1}^{3} x_i n_i$$

and

- <n> - Average number of sites per ring, (-).

Appendix C: Simple Analytical Isotherm Model

During the early years of ion exchange development an understanding of the important equilibrium processes were being pursued. A simple analytical model was proposed by Hale and Reichenberg (1949) where the deprotonation relationship that governs the hydrogen disassociation process within the resin phase was supplemented with a mass action ion exchange expression for addressing the resin-to-solution exchange process. In this appendix the analytical model of Hale and Reichenberg (1949) is provided. The success of this simple model was demonstrated by those authors for both monofunctional strong and weak acid resins (i.e., sulfonated cross-linked polystyrene and cross-linked polymethacrylic acid resin, respectively). We have used this simple analytical model for verification purposes in testing our more complicated and generic numerical model where through input similar conditions can be arrived at.

Note that this simple analytical model is limited to the following conditions:

- Monovalent cation exchange between one counter-ion and hydrogen;
- A resin containing only single site ionogenic groups; and
- Ion-exchange only (no neutral species absorption occurring).
- Disassociation of water not considered.

C.1 Ion-Exchange Relationship

Hale and Reichenberg (1949) focused their attention on the ion exchange of H^+ and Na^+. The exchange equilibrium between the resin phase and the aqueous solution is expressed using the following mass action process:

$$\overline{H}^+ + Na^+ \overset{K_N}{\leftrightarrow} \overline{Na}^+ + H^+ \qquad \text{(C-1)}$$

which in equation form becomes:

$$K_N = \frac{[H^+][\overline{Na}^+]}{[\overline{H}^+][Na^+]} \qquad \text{(C-2)}$$

where

- K_N - Ion exchange selectivity coefficient for the Na-H exchange process, (-).
- $[\overline{H}^+]$ - Concentration of disassociated H^+ ion within the resin phase, (mmol/ml).
- $[\overline{Na}^+]$ - Concentration of Na^+ ion within the resin phase, (mmol/ml).
- $[H^+]$ - Concentration of H^+ ion within the aqueous solution, (mmol/ml).
- Na^+ - Concentration of Na^+ ion within the aqueous solution, (mmol/ml).

Here activities are being approximated by their concentration values. The exchange process shown by Eq. (C-1) represents the exchange of Na ions in solution with disassociated H ions held within the resin phase. Undissociated H ions (i.e., RH) are not a part of this exchange equilibrium process. The selectivity coefficient, K_N, as defined by Eq. (C-2) is not a true thermodynamic constant since nonidealities and other effects will impact its value. Values for this selectivity coefficient are expected to be on the order of 1-2 for Na-H exchange processes.

C.2 One-Site Deprotonation Relationship

Following the same approach given in Appendix B, the ionization reaction for the resin (i.e., the disassociation of the one ionogenic group) can be expressed as:

$$RH \overset{K_1}{\leftrightarrow} R^- + \overline{H}^+ \tag{C-3}$$

where in equation form becomes:

$$K_1 = \frac{[R^-][\overline{H}^+]}{[RH]} \tag{C-4}$$

where

- K_1 - Ionization constant for the specified reaction.
- [RH] - Ring concentration with unionized ionogenic group, (mmol/ml).
- [R] - Ring concentration with ionized ionogenic group, (mmol/ml).

For disassociation reaction, such as Eq. (C-4), the ionization constant is typically provided within the literature in terms of a pKa value defined as:

$$pKa_i = -\log_{10} K_i$$

The valance charges have been omitted for clarity. Note that the standard state chosen for the resonates (i.e., ring states) is on a per gram of dry resin in its pure H-form. The specific volume for the resin in its saturated (wet) state where the uptake of water solvent has reached its equilibrium value is:

- $\underline{V}$ - Specific volume of resin phase in terms of milliliter per gram of dry resin in its pure H-form (ml/g_{resin}).

The total concentration of rings present can be related to the scientific weight capacity of the resin's ionogenic groups by:

$$[Q_T] = [R_T]\underline{V} \tag{C-5}$$

where

- Q_T - Scientific weight capacity of ionogenic groups ($mmol/ g_{resin}$).
- and here it has been assumed that only 1-site per available ring exists.

- R_T - Concentration of total rings present within resin phase that contains ionogenic groups (mmol/ml).

and

$$[R_T] = [RH] + [R^-] \tag{C-6}$$

An electro-neutrality balance (i.e., charge balance) on the resin imposes:

$$[R^-] = [\overline{H}^+] + [\overline{Na}^+] \tag{C-7}$$

C.3 Simple Analytic Model

Above the various necessary equations have been listed. Now, we shall solve for the Na loading held within the resin. The solution obtained is expressed in terms of the ratio of ions within the aqueous solution by:

$$x = \frac{[Na^+]}{[H^+]} \tag{C-8}$$

As shown by Hale and Reichenberg (1949) the exchange process is governed by this ratio and not independently by either ion concentration.

Rearranging Eqs. (C-2) and (C-4) yields:

$$[\overline{Na}] = xK_N[\overline{H}] \tag{C-9}$$

$$[\overline{H}] = K_1 \frac{[RH]}{[R]} \tag{C-10}$$

Combining these two equations:

$$[\overline{Na}] = xK_N K_1 \frac{[RH]}{[R]} \tag{C-11}$$

From Eq. (C-6), the total capacity implies:

$$[RH] = [R_T] - [R] \tag{C-12}$$

Using Eq. (C-9), Eq. (C-7) becomes:

$$[R] = \left\{1 + \frac{1}{xK_N}\right\}[\overline{Na}^+] \tag{C-13}$$

Expanding Eq. (C-11), substituting in Eqs. (C-12) and (C-13) yields:

$$[\overline{Na}] = xK_N K_1 \left\{ \frac{[R_T] - [\overline{Na}]\left\{1 + \frac{1}{xK_N}\right\}}{[\overline{Na}]\left\{1 + \frac{1}{xK_N}\right\}} \right\} \tag{C-14}$$

Rearranging Eq. (C-14):

$$\left\{1 + \frac{1}{xK_N}\right\}[\overline{Na}]^2 = [R_T]xK_N K_1 - xK_N K_1 \left\{1 + \frac{1}{xK_N}\right\}[\overline{Na}] \tag{C-15a}$$

or

$$[\overline{Na}]^2 + xK_N K_1 [\overline{Na}] - \left\{ \frac{[R_T]xK_N K_1}{\left\{1 + \frac{1}{xK_N}\right\}} \right\} = 0 \tag{C-15b}$$

Note that the solution to an equation of the form:

$$Ay^2 + By + C = 0 \tag{C-16a}$$

is given by

$$y = \frac{-B \pm \sqrt{B^2 - 4AC}}{2A} \tag{C-16b}$$

Thus, the solution to Eq. (15) becomes:

$$[\overline{Na}] = -\frac{xK_N K_1}{2} + \frac{xK_N K_1}{2} \sqrt{xK_N K_1 + \frac{[R_T]}{\left\{1 + \frac{1}{xK_N}\right\}}} \tag{C-17}$$

where the constraint of only positive roots implies only the + root is taken.

As stated earlier, Eq. (C-17) implies Na loading depends only on the ratio (x) and not on either [Na] or [H] independently. Note here the absence of a neutral salt such as NaCl or $NaNO_3$. Also, no attempt is made here to address the disassociation of water in the aqueous solution.

Appendix D: Simple Numerical Isotherm Model

As stated in Section 4.6 of the report, a simplified numerical isotherm model was employed to assist in developing a better understanding of the sRF resin over the entire pH range of expected column operations. The details of this model are provided within this appendix. This simple model adds to our foundation upon which more detailed and complete models are envisioned. Its success is illustrated in Section 4.6 of the report.

This model adds to our earlier work with the deprotonation model discussed in Appendix B and the simple analytic model discussed in Appendix C. Basically, Appendix B discusses the equations associated with deprotonation (sometimes referred to as ionization or disassociation) within the resin phase, while Appendix C includes a single mass action equation to reflect the ion exchange occurring between phases. In this appendix we add additional mass action equations to handle multi-ion exchange processes (i.e., selectivity).

We have limited the scope of this simple numerical model to the following conditions:

- Each group's electrochemical properties (i.e., expressed in terms of pK_a values) are independent of neighboring ring conditions. However, multiple sites on a given ring are addressed using multiple pK_a values.
- Steric effects are not being considered.
- No co-ion effects are being addressed such as the Donnan invasion of electrolyte.
- Only the counter-ions H^+, Na^+, K^+, and Cs^+ are considered.

Since this model is a basic proof of concept the following non-idealities and characteristics are not being considered at this time as well:

- Resin phase non-idealities such as activity coefficients of the resonates;
- Solution phase non-idealities such as activity coefficients of the electrolyte ions; and
- Swelling effects on resin due to solvation effects by water.

The first assumption above reflects our concept of an "ideal mixture" allowing us the ability to separate out the numerical problem into separate ones for each ring type individually. The actual resin behavior is then estimated by the summing up of the individual ring type behaviors using appropriately defined ring fraction input (i.e., the "ideal mixture" model).

D.1 Three-Site Deprotonation Relationships

For further details on deprotonation relationships see Appendix B. In our general case a ring type (i) can have up to three ionizable sites. As Appendix B illustrates, the ionization reactions for a 3-site ring can be expressed as:

$$RH_3 \overset{K_{1i}}{\leftrightarrow} RH_2^- + \overline{H}^+ \qquad \text{(D-1a)}$$

$$RH_2^- \overset{K_{2i}}{\leftrightarrow} RH^{-2} + \overline{H}^+ \qquad \text{(D-1b)}$$

$$RH^{-2} \overset{K_{3i}}{\leftrightarrow} R^{-3} + \overline{H}^{+} \quad \text{(D-1c)}$$

Let the various ring states be defined by the notation:

$$R_0 \equiv RH_3; \quad R_1 \equiv RH_2^{-}; \quad R_2 \equiv RH^{-2}; \quad R_3 \equiv R^{-3}$$

Then, the deprotonation relationships above can be expressed by the equations:

$$\left[R_1\right]\left[\overline{H}\right] = K_{1i}\left[R_0\right] \quad \text{(D-2a)}$$

$$\left[R_2\right]\left[\overline{H}\right] = K_{2i}\left[R_1\right] \quad \text{(D-2b)}$$

$$\left[R_3\right]\left[\overline{H}\right] = K_{3i}\left[R_2\right] \quad \text{(D-2c)}$$

For convention the first site is set to the ionogenic group with the lower pK_a value, the second to the intermediate value, etc.:

$$pKa_1 < pKa_2 < pKa_3$$

The formulation is set up within the Fortran algorithm such that a very large input value for the pK_{a3} value (i.e., say a value of 1000 or larger) results in a dissociation constant of zero (due to round-off). This results in eliminating the third site from the list of available sites. In effect this reduces the 3-site model automatically down to a 2-site model. Setting the pK_{a2} value to 1000+ further reduces the model down to a 1-site model.

Electroneutrality within the resin follows directly from the concentrations of the various ionic species held within the resin phase as:

$$\left[\overline{H}\right] + \left[\overline{Na}\right] + \left[\overline{Cs}\right] + \left[\overline{K}\right] = 0 \cdot \left[R_0\right] + 1 \cdot \left[R_1\right] + 2 \cdot \left[R_2\right] + 3 \cdot \left[R_3\right] \quad \text{(D-3)}$$

Note that each ring state differs from the others by one negative unit in charge. For example, as the ring state notation indicates, the subscript implies the number of negative charge units a ring state possesses.

The electroneutrality expression given by Eq. (D-3) is limited here to just the four counter-ions listed on the left-hand side of the equation. For additional counter-ions, corresponding terms would be added to the left-hand side. If neutral species were to be added to the model (e.g., NaCl) then co-ion terms would also be required on the right-hand side as well.

D.2 Ion-Exchange Relationship

The simple analytical isotherm model, as described in Appendix C, addresses only the ion exchange of H^+ and Na^+ between the resin and aqueous phases. Here the multi-cation exchange processes for H^+, Na^+, K^+, and Cs^+ are considered. Their mass-action (ion-exchange) relationships are expressed by:

$$\overline{H}^{+} + Na^{+} \overset{K_{Ni}}{\leftrightarrow} \overline{Na}^{+} + H^{+} \quad \text{(D-4a)}$$

$$\overline{H}^{+} + K^{+} \overset{K_{Ki}}{\leftrightarrow} \overline{K}^{+} + H^{+} \quad \text{(D-4b)}$$

$$\overline{H}^{+} + Cs^{+} \overset{K_{Ci}}{\leftrightarrow} \overline{Cs}^{+} + H^{+} \quad \text{(D-4c)}$$

Here we limit our focus for now by assuming electrochemical and steric effects are not impacting rings locally (e.g., ring states like RH-Na-K versus RH-Na_2 are assumed similar).

These relationships can be expressed in equation form as:

$$K_{Ni} = \frac{[H^{+}][\overline{Na}^{+}]}{[\overline{H}^{+}][Na^{+}]} \quad \text{(D-5a)}$$

$$K_{Ki} = \frac{[H^{+}][\overline{K}^{+}]}{[\overline{H}^{+}][K^{+}]} \quad \text{(D-5b)}$$

$$K_{Ci} = \frac{[H^{+}][\overline{Cs}^{+}]}{[\overline{H}^{+}][Cs^{+}]} \quad \text{(D-5c)}$$

where

- K_{Ni} - Ion exchange selectivity coefficient for the Na-H exchange process, (-).
- K_{Ki} - Ion exchange selectivity coefficient for the K-H exchange process, (-).
- K_{Ci} - Ion exchange selectivity coefficient for the Cs-H exchange process, (-).
- $[\overline{H}^{+}]$ - Concentration of disassociated H^{+} ion within the resin phase, (mmol/ml).
- $[\overline{Na}^{+}]$ - Concentration of Na^{+} ion within the resin phase, (mmol/ml).
- $[H^{+}]$ - Concentration of H^{+} ion within the aqueous solution, (mmol/ml).
- Na^{+} - Concentration of Na^{+} ion within the aqueous solution, (mmol/ml).

Note that the selectivity coefficients for the various other exchange processes (e.g., Cs-Na exchange) are not independent and can be derived from the above Eqs. (D-4 and D-5). For example the Cs-H ion exchange equations become:

$$\overline{Na}^{+} + Cs^{+} \overset{K_{CNi}}{\leftrightarrow} \overline{Cs}^{+} + Na^{+} \quad \text{(D-6)}$$

$$K_{CNi} \equiv \frac{[Na^{+}][\overline{Cs}^{+}]}{[\overline{Na}^{+}][Cs^{+}]} = \frac{K_{Ci}}{K_{Ni}} \quad \text{(D-7)}$$

Here activities are being approximated by their concentration values. The exchange process shown by Eq. (C-1) represents the exchange of Na ions in solution with disassociated H ions held within the resin phase. Undissociated H ions (i.e., RH) are not a part of this exchange equilibrium process. The selectivity coefficient, K_N, as defined by Eq. (C-2) is not a true thermodynamic constant since nonidealities and other effects will impact its value. Values for this selectivity coefficient are expected to be on the order of 1-2 for Na-H exchange processes.

D.3 Resin Capacity

The total concentration of rings (both unionized and ionized) becomes (i.e., four types of ring states):

$$[R_T] = [R_0] + [R_1] + [R_2] + [R_3] \tag{D-8}$$

The total concentration of rings present can be related to the scientific weight capacity of the resin's ionogenic groups by:

$$[Q_T] = 3[R_T]\underline{V} \tag{D-9}$$

where

- Q_T - Scientific weight capacity of ionogenic groups (mmol/ g_{resin}).
  and here it has been assumed that only 3-sites per available ring exist.
- R_T - Concentration of total rings present within resin phase that contains
  ionogenic groups (mmol/ml).
- $\underline{V}$ - Specific volume of resin phase in terms of milliliter per gram of dry resin in
  its pure H-form (ml/g_{resin}).

D.3 Solution Approach

The above set of equations define the equilibrium state of a given resin type (i) when in contact with a large and specified aqueous phase solution. The variables under consideration are:

- within the resin phase: $[\overline{H}^+],[\overline{Na}^+],[\overline{K}^+],[\overline{Cs}^+],[R_0],[R_1],[R_2],[R_3]$
- within the aqueous phase: $[H^+],[Na^+],[K^+],[Cs^+]$

There are 8 eight equations and 12 variables. We must specify 4 variables for a unique solution and based on the "ideal" mixture model approach we are specifying the 4 aqueous phase concentrations. This setup resembles a numerical batch contact analysis (i.e., similar in nature as employed in CERMOD) where the phase ratio (i.e., solution volume to resin material) is assumed to be infinite.

As discussed within Appendix B, the mixture isotherm for the actual resin is then computed based on an appropriately weighted sum of the computed isotherms for each resin type within the resin. We define the mixture resin by specifying the number fractions of ring types present:

$$x_i \quad (i = 1,2,3)$$

where

- x_i - Number fraction of available ring types within resin (i.e., total number of rings of type i per total number of all available rings present).

The number of rings of a given ring type becomes:

$$[R_i] = x_i[R_T] \quad (i = 1,2,3) \tag{D-10}$$

where

- $[R_i]$ - Number rings of type i per ml of resin, (mmol/ml).
- $[R_T]$ - Total number of available rings within the resin per ml, (mmol/ml).

D.4 Required Input

In order to generate a composite isotherm for a polyfunctional resin the following input parameters must be provided:

Number of ring types (1, 2, or 3)

Total scientific weight capacity

Number of available sites per ring type (1, 2, or 3)

Number fractions of ring types (sums to unity)

pK_a values for each site on each ring type

Selectivity coefficients for each ion-exchange pair for each ring type

As an example, below the input decks for the results shown in the main body of the report are listed for the Resorcinol-benzaldehyedisulfonic acid-formaldehyde resin tested by Topp and Pepper (1949). The case shown below is where it is assumed that the resin is made up of 2 ring types: (1) one containing a single-site ring of the nuclear sulfonic ionogenic group and the other ring containing 2-sites of one carboxylic group plus 2 resorcylic groups.

The Ionogenic Group Data Record:

```
/ntypes   Qt/
 2       9.
/nsites/
 1  3
/xfrac/
 0.5   0.5
/pKa(i,j)   pKa(i,j)   pKa(i,j), i=1,max(nsites), j=1,ntypes/
-1.00d+0    1.00d+3    1.00d+3   ! nuclear     SO3H-
 5.500+0    9.00d+0    1.13d+1   ! carboxcylic COOH- + resorcylic  OH-
```

The Mass Action Data Record:

```
/nmae/
 3
/Ks(i,j), i=1,nmae, j=1,ntypes/
/Na+/H+   K+/H+    Cs+/H+     /
 0.00     2.50     0.00   ! sulfonic SO3H-
 0.00     1.00     0.00   ! carboxcylic COOH- + resorcylic  OH-
```

Distribution:

S. E. Aleman, 735-A
J. V. Odum, 735-A
S. J. Hensel, 703-41A
L. L. Hamm, 703-41A
F. G. Smith, III, 703-41A
W. D. King. 773-42A
C. A. Nash, 773-42A
F. M. Pennebaker, 773-42A
A. P. Fellinger, 773-42A
W. R. Wilmarth, 773-A
S. L. Marra, 773-A